Plant material

Lunularia cruciata (*Lunularia*) culture was isolated in the Pyrennées moutains (France) and cultured *in vitro* on M medium (1). *Closterium peracerosum-strigosum-littorale complex* (strain NIES-67 - *Closterium*) was provided by the NIES (http://mcc.nies.go.jp/02introduction-e.html) and grown in MBL medium (2) at 20/24°C (16H light). *Spirogyra sp.* was cultivated in liquid 3N-BBM+V medium and kept shaking at 25 °C with a speed of 60 rpm as described previously (Delaux et al. 2012). *Medicago truncatula* wild-type and *ccamk-1* (TRV25) mutants, both in the Jemalong A17 background were used.

Treatment of *Lunularia* and *Closterium*

Lunularia cruciata young thallus produced from gemmae were inoculated with 100 spores of *Rhizophagus irregularis* (AM) or water (Mock) on M medium (3) and incubated at 20/24°C (16H light). Plants were collected after two month and frozen in liquid nitrogen before RNA extraction. Three weeks-old *Closterium* cultures were divided in 6 flasks (25ml culture in 125ml flasks) and treated for 24 hours with exudates of *Rhizophagus irregularis* (final concentration 400 spores/ml), generated as previously (4), or with water. Samples were then collected by centrifugation (1 min, 8,000g) and frozen in liquid nitrogen.

***Lunularia* and *Closterium* RNA extraction**

Frozen samples were grinded in liquid nitrogen and total RNA was extracted using RNeasy plant mini kit (Qiagen) following the manufacturer's recommendations. RNA quantification was performed by Nanodrop. RNA quality was assessed on Agilent Bioanalyzer. Samples with RNA integrity Number (RIN) higher than eight were selected.

Construction of RNA Seq Libraries for *Lunularia* and *Closterium*

Each RNA library was generated following Illumina TruSeq RNA Sample Preparation Guide and the Illumina TruSeq RNA Sample Preparation Kit (Illumina Inc., San Diego, California, USA). mRNA was purified from 1ug total RNA using poly-T oligo-attached magnetic beads. Subsequently, each mRNA sample was fragmented using divalent cations under elevated temperature, and purified. Double-stranded cDNAs were synthesized using SuperScript II (Invitrogen, Carlsbad, California, USA) Reverse Transcriptase and random primers for first strand cDNA synthesis followed by second strand synthesis using DNA Polymerase I and RNAseH for removal of mRNA. Double-stranded cDNA was purified using Agencourt AMPure XP beads (Qiagen, Valencia, California, USA) as recommended in the TruSeq RNA Sample Prep Guide. cDNAs were end-repaired by T4 DNA polymerase and Klenow DNA Polymerase, and phosphorylated by T4 polynucleotide kinase. The blunt ended cDNA was purified using Agencourt AMPure XP beads. The cDNA products were incubated with Klenow DNA Polymerase to add an 'A' base (Adenine) to the 3' end of the blunt phosphorylated DNA fragments and then purified using Agencourt AMPure XP beads. DNA fragments were ligated to Illumina adapters, which have a single 'T' base (Thymine) overhang at their 3'end. The adapter-ligated products were purified using Agencourt AMPure XP beads. Adapter ligated DNA was amplified in a Linker Mediated PCR reaction (LM-PCR) for 13 cycles using Phusion^{TM} DNA Polymerase and Illumina's PE genomic DNA primer set followed by purification using Agencourt AMPure XP beads. Quality and quantity of finished libraries were assessed using an Agilent DNA1000 series chip assay (Agilent Technologies, Santa Clara, CA) and Invitrogen Qubit HS Kit (Invitrogen, Carlsbad, California, USA), respectively. Each library was standardized to 2μM. For samples of *Lunularia cruciata* colonized by *Rhizophagus irregularis*, twelve cycles of PCR were applied to amplify libraries, and size selection was performed on E-gel (Invitrogen). Libraries were quantified by qPCR using the KAPA Library Quantification Kit (PN11 KK4824).

RNA sequencing

Cluster generation was performed using a TruSeq Single Read Cluster Kit (v3) and the Illumina cBot, with libraries multiplexed for 1x100bp sequencing using the TruSeq 100bp SBS kit (v3) and HCS1.6 software, on an Illumina HiSeq2000. Images were analyzed using CASAVA. For *Lunularia cruciata* colonized by Rhizophagus irregularis, RNA-seq experiments were performed on an Illumina HiSeq2000, using a paired-end read length of 2 x100 bp with the Illumina TruSeq SBS sequencing kits v3 (PN FC-401-3001, HiSeq2000). Data have been generated from paired-end libraries (2x100 bp) with insert sizes ranging from 200 to 300 bp. Sequencing was performed at the GeT-PlaGe platform (https://genomique.genotoul.fr, Toulouse, France). In addition, 454 pyrosequencing was performed on colonized tissues. Approximately 0.5 µg of total RNA was used for construction of Roche 454 GS FLX sequencing library following the manufacturer's protocol. Libraries were sequenced using one-eighth of Pico Titer Plate. All sequenced reads have been submitted at the National Center for Biotechnology Information's Sequence Read Archive (accession nos. SRR1027885).

Closterium assembly

Raw data from 15 libraries containing a total of 404,421,355 raw Illumina 100bp single-end reads (~ 40 Gbp) were pooled for *de novo* transcriptome assembly. The fastx-toolkit v.0.0.13 (Hannon lab, Cold Spring Harbor) was used for quality assessment and TruSeq adapter trimming. Assembly was performed using the Trinity assembler version r20140413p1 with the following modified parameters: "--PasaFly –normalize_reads --min_kmer_cov 3 --trimmomatic --quality_trimming_params "LEADING:5 TRAILING:5 MINLEN: (5). The assembly produced 119,254 contigs representing 83,700 "gene units" (based on Trinity determination). The average contig length was 866 nt, with 65,495 contigs >= 500 nt and 10,506 contigs >= 2,000 nt. Unprocessed read data is deposited at the NCBI Short Read Archive (PRJNA296352).

***Lunularia* assembly**

To define the gene repertoire of *Lunularia,* a transcriptome assembly was generated by using the CLC Genomic Workbench suite (v7.0, CLC Bio, Denmark). We choose a strategy combining 500-bases-long reads from 454 pyrosequencing data and 100 base-long reads Illumina data. We mixed sequences obtained from *Lunularia* thallus associated or not to *R. irregularis*. Pyrosequencing data were performed on mycorrhizal thalli and generated 138,245 reads (51,920,771 nucleotides; mean 492 bases). Two optima of GC contents were observed, 28 and 48%, the first one being characteristic of *R. irregularis* (6). The fungal–originating reads were eliminated by mapping reads on the genomes of *R. irregularis* (Gloin1 and Rir sequences, (6, 7)) using CLC mapping tool. Illumina single reads (100 bp from Hiseq2000) were obtained from six libraries of RNA from non mycorrhizal thalli, leading to 173,377,946 reads (17.5 Gb). The resulting reads were trimmed based on the quality scores (limit: 0.05) and end ambiguity based on adaptor sequences used for librairies (maximum number of ambiguities: 2). The reads less than 50bp long after trimming were discarded. The trimmed and filtered reads from 454 and Illumina were de novo assembled into contigs using CLC software with default setting. The resulting assembly (Luc_v1; available at www.polebio.lrsv.ups-tlse.fr/Luc_v1/) is formed by 70,122 contigs (av. length 781; max length 22,117; N50= 1,275). Luc_v1 assembly was used for further annotation and gene expression analysis.

***Lunularia* gene expression analysis**

For gene expression analysis, we used additional triplicates Illumina libraries from mock and symbiotic samples (*Lunularia* and *Lunularia* + *R.irregularis*). Reads were mapped to the Luc_v1 assembly to calculate gene expression using CLC Genomic Workbench suite. To find genes significantly up-regulated during symbiosis, RPKM and proportion-based test statistics with a False Discovery Rate (FDR) correction for multiple testing were calculated (settings: minimum mapped read length fraction = 0.95; minimum similarity = 0.98). According to CLC recommendation, genes were considered as significantly up regulated when meeting the

requirements of "total difference reads mapped" >10, RPKM fold change>2 and FDR corrected p-value<0.05.

Spirogyra DNA extraction

Spirogyra sp. (AU1) was chosen for the genomic sequence Genomic DNA was extracted from fresh materials with adapted CTAB method (8). Spirogyra filaments were collected by filtration and disrupted in the CTAB buffer with a bead beater.

Spirogyra sequencing and assembly

The genomic sequence was launched with Illumina MiSeq sequencer and HiSeq sequencer. Before loading the genomic DNA on the sequencer, fragmentation together with adaptor incorporation (tagmentation), limited-cycle PCR amplification, and size selection were performed to make size-specific DNA libraries compatible with Illumina sequencers. The sizes of insertions obtained with HiSeq and MiSeq methods were 426 bp and 502 bp respectively. FASTQC Toolkit version 0.10.1 was used to check and evaluate the raw data quality (9). The assembly process was performed with SOAPdenovo version 2.04 (10) following a length adjustment process with Flash (fast length adjustment of short reads) (11). Sequence assembly is deposited at the NCBI BioProject depository (Submission ID: SUB1029739 / BioProject ID: PRJNA290461)

Plasmid construction

To clone *Closterium peracerosum-strigosum-littorale complex CCaMK* (*CpCCaMK*) cDNA were generated (Fermentas) from 500ng of DNAse-treated (Ambion) RNA extracted as described above. 1 µl was used in a PCR reaction using primers 5'-CACCATGGGCGACGTGGAGGAG-3' and 5'- TCACCACTGATGTTGCCGGAAT-3'. *Cp-CaCBD* was generated by PCR from *CpCCaMK*. First, two PCR were conducted in parallel; PCR1: primers Cp-CaCBD-GAT-F1 5'-CACCATGGGCGACGTGGAGGA-3' and CaM-CaCBD-R1 5'-

ACGCTGCGGAATTTCTTCTTCGCATTCAAGGTGAGCAGGCGCCGGCACA-3'. PCR2: Cp-CBD-GAT-R1 5'-TCACCACTGATGTTGCCGGAAT-3' and CaM-CaCBD-F1 5'-GAAATTCCGCAGCGTTGGTTTCGCGGTGATCGTGAGCAACAAGCTCATGC-3'. After purification of the PCR products, one µl of each was used for PCR3, at 50°C for 5 cycles. Then, primers Cp-CaCBD-GAT-F1 and Cp-CBD-GAT-R1 were added to the PCR reaction and 30 more cycles at 62°C were performed. Gel purified PCR products were cloned in pENTR D TOPO (Invitrogen). After sequencing, pENTR CpCCaMK and CpCaCBD were transferred to pVP16 by LR reactions (Invitrogen) to generate "Maltose Binding Protein"(MBP)-CpCCaMK and MBP-Cp-CaCBD fusions for protein purification. pENTR CpCCaMK and pENTR Cp-CaCBD were then used to generate 35S:*CpCCaMK* and *35S:Cp-CaCBD* by recombination in a pK7FWG2-RR vector. This vector allows constitutive expression of DsRED as a transformation marker. *Chlamydomonas reinhardtii* (CrCDPK1 - Cre33.g782750) and *Chlorella variabilis* (CvCDPK3 - Cva20239) *CDPKs* genes were synthesized by Biomatik with *Sal*I and *Not*I restriction sites added on the 5' and 3' ends respectively. Both CDPKs were then digested with *Sal*I and *Not*I, cloned in pENTR1A and transferred in pVP16 by LR recombination, resulting in MBP-CrCDPK and MBP-CvCDPK fusions. *Chlorokybus atmophyticus* and *Nephroselmis pyriformis* CCaMK were synthesized by Life Technology with *Bsa*I sites and overhangs to use them as level-0 in GoldenGate cloning, accordingly to the standards for plant synthetic biology (12). First, level 1 modules were generated by fusing a 35S promoter and terminator to CaCCaMK and NpCCaMK, in the R2 backbone (13). Another level-1, with the fluorescent reporter DSred under control of the *Arabidopsis* thaliana Ubiquitin promoter and a 35S terminator was generated in a R1 level-1 backbone. The L1M-R2-p35S-CaCCaMK-t35S or L1M-R2-p35S-NpCCaMK-t35S modules where then cloned in position two of a Level-2 backbone with L1M-R1-pAtUBI-DSred-t35S in position 1, accordingly to patron (13).

Medicago root transformation and Mycorrhization assays

Roots of *Medicago truncatula* A17 or *ccamk-1* mutant (TRV25) in the A17 background (14) were transformed using *Agrobacterium rhizogenes* AR1193 following (15). Three weeks after transformation, roots were checked for red fluorescence under a dissecting scope. Plants with positive roots were transferred to 30ml pots inoculated with 1/15 of Solrize Pro (Agrauxine, France) in a mix of sand and clay. After 5 weeks of incubation at 21°C (16H light) plants were collected and transgenic roots (*i.e.* showing red fluorescence) were harvested under a dissecting scope (Figure S21A). Mycorrhization level was quantified using the grid intersect method.

RNA extraction and RT-PCR

Roots were collected as described previously and immediately frozen in liquid nitrogen after collection under microscope. RNA was extracted using the Qiagen RNAeasy extraction kit. RNA were treated with DNAse (Ambion) and 1 ug used to generated cDNA. cDNA were generated with Qiagen superscriptIII. For PCR, 0.5 ul of cDNA were used for each sample with primers MtPT4-F 5'-GACACGAGGCGCTTTCATAGCAGC-3' and MtPT4-R 5'-GTCATCGCAGCTGGAACAGCACCG-3' for *MtPT4* and MtUbi-F 5'-GCCGGAAAACAGCTAGAAGA-3' and MtUbi-R 5'-GGAGACGGAGAACAAGGTGA-3' for *MtUBIQUITIN*. The same cDNA were used to test for expression of the transgenes using primers in Figure S21B, C.

Protein extraction and purification

pVP16 vectors containing *CpCCaMK*, *CrCDPK*, *CvCDPK* or *MtCDPK* were transformed in *E. coli* Rosetta strain. Single colonies were grown overnight in LB supplemented with Ampicillin (Sigma). 50 ml of LB in a 250 ml flask were then inoculated with 1.25ml of the overnight cultures. Once OD_{600nm} reached 0.5, 0.5 mM isopropyl-b-D-1-thiogalactopyranoside was added. 4 hours after induction the cultures were pelleted at 4°C and suspended in 5 ml of extraction buffer (20 mM HEPES pH7.4, 300 mM NaCl, 5 mM MgCl2, 10% Glycerol, 2mM Mercaptoethano) in 50 ml

conical tubes. The solutions were sonicated for 15 seconds three times and 500 µl of Triton X100 added. After 15 minutes centrifugation at 4°C, the supernatant was mixed with 500 µl of 50% slurry of rinsed (1X PBS) Amylose resin (New-England Biolab) and incubated for at least two hours at 4°C with slow shacking. Beads were then washed three times with PBS 1X and eluted with 300 µl 10mM Maltose in 10mM Tris-HCl pH 7.2 (1000G for 5 minutes). Protein extracts were stored at -80°C.

Calmodulin binding assays

Calmodulin from bovine testis (Sigma-Aldrich) was labeled with biotin using ECL Protein Biotinylation Module (GE Healthcare). A polyvinylidene difluoride membrane (Immun-Blot, Rio-Rad) was rinsed with Methanol for two minutes and incubated in TBS 1X (50 mM Tris-HCl, 150 mM NaCl) for 20 minutes. 5 µl of purified CCaMK and CDPK proteins at 100 ng/µl were spotted and the membrane was blocked in Blocking solution (TBS 1X, 0.1% Tween 20, 5% skim milk) at room temperature for 1 hour. The membrane was then incubated overnight with 100 ng/mL biotinylated Calmodulin in Binding buffer (TBS 1X containing 1 mM $CaCl_2$ or 5 mM EGTA) at 4°C. After several washes in Rinsing solution (TBS 1X, 0.1% Tween 20, 1 mM $CaCl_2$ or 5 mM EGTA) the membrane was incubated with streptavidin-conjugated horseradish peroxidase in binding buffer at room temperature for 1 h. Binding of biotinylated CaM to CCaMK was detected by ECL Plus Western Blotting Detection Reagents (GE Healthcare).

***In vitro* kinase assays**

Kinase assays were performed as described in (16). 5 µg MBP-CCaMK protein (0.5 µg for assays with Calmodulin) were incubated in Kinase buffer (50 mM HEPES, pH 7.5, 1 mM DTT, 200 µM ATP, and 5 µCi [g-^{32}P]ATP, 10 mM $MgCl_2$) 20 µL reaction at 30°C for five or ten minutes, in presence of 0.2 mM $CaCl_2$ (+Ca^{2+}) or 2.5 mM EGTA (+EGTA). For assays with Calmodulin 0.5 µM bovine Calmodulin (Millipore) was added. The reactions were terminated by

boiling at 95°C for 5 min. Samples were then separated by 10% SDS-PAGE. The radioactivity was quantified by Molecular Dynamics Storm® 860 phosphorimager (Sunnyvale, CA) and data were analyzed using the Molecular Dynamics ImageQuant® software.

Extended dataset

The detailed list of genomes and transcriptomes used for the phylogenetic analysis is provided in Dataset S1. Except for *Lunularia* and *Closterium* transcriptomes all the transcriptomes used were generated by the One Thousand Plant Project (http://onekp.com/project.html). Details for RNA extraction, sequencing and assemblies are available in (17).

Sequence collection

Prediction of the amino acid sequences for the new assemblies of *Closterium*, *Lunularia* and *Spirogyra sp.* and for the recently published assemblies of *Nitella mirabilis*, *Mesostigma viride*, *Spirogyra sp* and *Coleochaete orbicularis* was done using the AUGUSTUS package using the parameter set defined for *Arabidopsis thaliana* (18). Using the combined amino acid dataset from these sources, putative homologs of the various genes used in this study were extracted by using the HMMER package (http://hmmer.org) and the respective PFAM domains (http://pfam.xfam.org) present in each of the families to which these proteins belong (19, 20). The domains in each of these families used for the searches were: LysM-RLKs [PF01476, PF00069], GRAS [PF03514], DMI1 [PF06241], CDPKs [EF-hand, PF00069], VAPYRIN [PF00635,CL0465], and RAM2 [PF12710,PF01553]. Sequences were then de-duplicated and used for further analyses. For the GRAS family, sequences that had a GRAS domain were further filtered by checking for the presence of the LHRII, PFYRE and SAW motifs characteristic of all known GRAS proteins to avoid the use of fragmented sequences. Presence of the domains was confirmed for all the proteins using InterProScan (http://www.ebi.ac.uk/interpro/). For the phosphate transporter, ABCG and the H+-ATPase families, BLASTp search was conducted

using the full-length protein from *Medicago* as query to reduce the number of sequences. The best equal hits were selected. For IPD3, BLASTp search was conducted using the highly conserved C-terminal domain. For each gene, size distribution of the collected was determined and short outliers removed. These outliers were blasted on the *Medicago* genome to determine if they could belong to the clade of interest (reciprocal blast, with initial query in the first equal hits). This was the case for *Lunularia* RAM1 and *Amborella* PT4.

Phylogenetic analysis

All the potential homologs were aligned using MAFFT (http://mafft.cbrc.jp/alignment/server/) and the alignment curated using BioEdit. For each gene family, Maximum likelihood trees were constructed with RAxML version 8.1.22 (21, 22). First substitution models were determined using the program parameter "PROTGAMMAAUTO", optimal models were: LG for CDPK, DMI1, GPAT, H^+-ATPase, PT, ABCG and Vapyrin; JTT for GRAS and IPD3; WAG for LysM-RLK and MLD-RLK. We used 10 different starting trees on a given alignment using the parsimonator algorithm of RAxML with 10 different random seeds. We estimated 10 maximum likelihood analyses on different starting trees. Next, we conducted the standard bootstraps and performed ML analysis on 100 replicates. Finally, we selected the tree with best likelihood score and drew bootstrap supports onto each selected tree. The newick-formatted trees were read and processed using the *ETE2* library (23) and the scripts were written in Python 2.7.9 for bioinformatics analysis. The clades of interest were then extracted from the larger tree, re-aligned and a Maximum-likelihood tree built using MEGA6 (24) and the substitution models define by RaxML. 100 bootstraps were conducted. Short sequences removed before building the initial phylogeny were included in these targeted analyses.

References

1. Delaux PM*, et al.* (2012) Origin of strigolactones in the green lineage. *New Phytol*. 195(4):857-871

2. Nichols H (1973) *Handbook of Phycological Methods* (Cambridge University Press).
3. Bécard G & Piché Y (1989) Fungal Growth Stimulation by CO(2) and Root Exudates in Vesicular-Arbuscular Mycorrhizal Symbiosis. *Appl Environ Microbiol* 55(9):2320-2325.
4. Mukherjee A & Ané JM (2011) Germinating spore exudates from arbuscular mycorrhizal fungi: molecular and developmental responses in plants and their regulation by ethylene. *Mol Plant Microbe Interact* 24(2):260-270.
5. Grabherr MG*, et al.* (2011) Full-length transcriptome assembly from RNA-Seq data without a reference genome. *Nat Biotechnol* 29(7):644-652.
6. Tisserant E*, et al.* (2013) Genome of an arbuscular mycorrhizal fungus provides insight into the oldest plant symbiosis. *Proc Natl Acad Sci U S A* 110(50):20117-20122.
7. Lin K*, et al.* (2014) Single nucleus genome sequencing reveals high similarity among nuclei of an endomycorrhizal fungus. *PLoS Genet* 10(1):e1004078.
8. Winnepenninckx B, Backeljau T, & De Wachter R (1993) Extraction of high molecular weight DNA from molluscs. *Trends Genet* 9(12):407.
9. Patel RK & Jain M (2012) NGS QC Toolkit: a toolkit for quality control of next generation sequencing data. *PLoS One* 7(2):e30619.
10. Luo R*, et al.* (2012) SOAPdenovo2: an empirically improved memory-efficient short-read de novo assembler. *Gigascience* 1(1):18.
11. Magoč T & Salzberg SL (2011) FLASH: fast length adjustment of short reads to improve genome assemblies. *Bioinformatics* 27(21):2957-2963.
12. Patron NJ (2014) DNA assembly for plant biology: techniques and tools. *Curr Opin Plant Biol* 19:14-19.
13. Engler C*, et al.* (2014) A golden gate modular cloning toolbox for plants. *ACS Synth Biol* 3(11):839-843.
14. Lévy J*, et al.* (2004) A putative Ca2+ and calmodulin-dependent protein kinase required for bacterial and fungal symbioses. *Science* 303(5662):1361-1364.
15. Boisson-Dernier A*, et al.* (2001) Agrobacterium rhizogenes-transformed roots of Medicago truncatula for the study of nitrogen-fixing and endomycorrhizal symbiotic associations. *Mol Plant Microbe Interact* 14(6):695-700.
16. Miller JB*, et al.* (2013) Calcium/Calmodulin-dependent protein kinase is negatively and positively regulated by calcium, providing a mechanism for decoding calcium responses during symbiosis signaling. *Plant Cell* 25(12):5053-5066.
17. Johnson MT*, et al.* (2012) Evaluating methods for isolating total RNA and predicting the success of sequencing phylogenetically diverse plant transcriptomes. *PLoS One* 7(11):e50226.
18. Stanke M, Steinkamp R, Waack S, & Morgenstern B (2004) AUGUSTUS: a web server for gene finding in eukaryotes. *Nucleic Acids Res* 32(Web Server issue):W309-312.
19. Finn RD, Clements J, & Eddy SR (2011) HMMER web server: interactive sequence similarity searching. *Nucleic Acids Res* 39(Web Server issue):W29-37.
20. Finn RD*, et al.* (2014) Pfam: the protein families database. *Nucleic Acids Res* 42(Database issue):D222-230.
21. Stamatakis A (2014) RAxML version 8: a tool for phylogenetic analysis and post-analysis of large phylogenies. *Bioinformatics* 30(9):1312-1313.
22. Stamatakis A (2006) RAxML-VI-HPC: maximum likelihood-based phylogenetic analyses with thousands of taxa and mixed models. *Bioinformatics* 22(21):2688-2690.
23. Huerta-Cepas J, Dopazo J, & Gabaldón T (2010) ETE: a python Environment for Tree Exploration. *BMC Bioinformatics* 11:24.
24. Tamura K, Stecher G, Peterson D, Filipski A, & Kumar S (2013) MEGA6: Molecular Evolutionary Genetics Analysis version 6.0. *Mol Biol Evol* 30(12):2725-2729.

Supplementary Figures Legends

Appendix S1. Detailed Material and method

Figure S1. Maximum-likelihood tree of the LysM-domain containing receptor-like kinases identified in the extended dataset.

Figure S2. Maximum likelihood tree of the malectin-like ecto-domain (MLD) receptor like kinases

Figure S3. A) DMI2 is composed by a malectin-like ecto-domain (MLD) and a kinase. DMI2 evolved via duplication in land-plants. Maximum-likelihood tree of the DMI2 clade is presented. The entire MLD-Kinase tree is available in Figure S2. B) The orthologs of Medicago DMI2 found in liverworts display the same domain organization.

Figure S4. Maximum-likelihood tree of the DMI1 homologs. The colored boxes on the right indicate the conservation of the filter domain (ADAGNHA in Medicago DMI1). Black, blue and white squares indicate identical, homologous and different amino acids respectively.

Figure S5. Maximum-likelihood tree of the Calcium dependent protein kinases identified in the extended dataset. The colored boxes on the right indicate the conservation of the calmodulin binding domain domain (QMDPEIVSRLQSFNARRKLRAAAIASVWS in Medicago CCaMK). Black, blue and white squares indicate identical, homologous and different amino acids respectively.

Figure S6. A) Maximum-likelihood tree of IPD3. IPD3 appeared in advanced charophytes and is conserved as a single copy gene in land plants. B) IPD3 is composed by two main domains, a DNA-binding domain located at the N-terminus and an activation domain. Among these two domains, the DNA binding domain is the most conserved, especially in charophytes.

Figure S7. Charophyte proteins ortholog to the land plant LysM-RLK display a similar do;ain organization.

Figure S8. A) CpCCaMK display the same organization than MtCCaMK with a kinase domain at the N-terminus and EF-hands on the C-terminus. B) The auto-phosphorylation site, analogous to T271 in MtCCaMK, and to T265 in *Lotus japonicas* CCaMK, is conserved (S242) C) *Top left:* A structural model was predicted as previously for MtCCaMK (Miller et al. 2013). *Top right:* In absence of auto-phosphorylation a single hydrogen-bound is formed with E291. *Bottom left:* Mimicking a phosphorylation of S242 results in the formation of a hydrogen-bond with R245, similar to what is observed for MtCCaMK. *Bottom right:* Furthermore, mimicking a phosphorylation of S243 improve this network by forming three hydrogen-bonds with R295 and C215. D) Autophosphorylation assay of CpCCaMK. Like MtCCaMK, autophosphorylation of CpCCaMK is promoted by the presence of calcium (Ca^{++}). E) Effect of calmodulin on CpCCaMK auto-phosphorylation. Similarly to MtCCaMK, auto-phosphorylation of CpCCaMK is reduced in presence of calmodulin.

Figure S9. A) The calmodulin binding domain of *Closterium CCaMK* (CpCCaMK) and *Chlorokybus atmophyticus* CCaMK (CaCCaMK) are divergent. A chimeric protein Cp-CaCBD corresponding to CpCCaMK with 8 mutations mimicking the calmodulin binding domain of CaCCaMK was generated by PCR and called Cp-CaCBD (see Appendix S1). B) The ability of Cp-CaCBD to bind calmodulin was strongly reduced but not abolished (the original plot is available Figure S20). C) Trans-complementation assays of *Mtccamk-1* TRV25 mutant. Letters indicate statistically supported groups according to ANOVA and TuckeyHSD tests (P-values < 0.01). *Ccamk-1* roots expressing Cp-CaCBD were colonized to a level not distinguishable from the wild-type transformed with an empty vector (EV). D) Representative picture of WGA-FITC stained AM fungi colonizing plant roots of *ccamk-1* mutant expressing Cp-CaCBD. Bar= 100 um. E) Expression of the symbiotic phosphate transporter *MtPT4* was observed in colonized roots of *ccamk-1* transformed with Cp-CaCBD. F) Hyphopodium formed on *ccamk-1* roots expressing Cp-CaCBD resulted in a normal level of internal hyphae and arbuscules.

Figure S10. A) The auto-phosphorylation site analogous to MtCCaMK T271, and *Lotus japonicas* CCaMK T265, is conserved in angiosperms (red vertical line), lycophytes (yellow), mosses (light-green), liverworts (dark-green) and most advanced charophytes (dark-blue). Few advanced charophytes display a Cysteine instead, the impact of this mutation has not been investigated. Amino-acids that cannot be phosphorylated are present in basal-charophytes (dark-blue light-blue) and in chlorophytes (light-blue). B) *Top left:* A structural model was predicted for *Nitella mirabilis* CCaMK as previously for MtCCaMK (Miller et al. 2013) and CpCCaMK (Figure S8). *Top right:* In absence of auto-phosphorylation two hydrogen-bounds are formed with E287. *Bottom left:* Mimicking a phosphorylation of S238 results in the formation of a third hydrogen-bond with R291. *Bottom right:* mimicking a phosphorylation of the neighbouring T239 resulted in a single H-bond between S238 and R291. C) and D) Structural modelling of *Chlorokybus atmophyticus* and *Mesostigma viride* CCaMK confirmed the absence of H-bond network similar to *bona fide* CCaMK.

Figure S11. Maximum-likelihood tree of the GRAS transcription factors.

Figure S12. Maximum-likelihood tree of the ABC transporter, subfamily G, identified in the extended dataset.

Figure S13. A) Maximum-likelihood phylogenetic tree of STR and STR2 extracted from the ABC, subfamily G, transporter tree on the left. High-resolution image of the ABCG tree is available in Figure S12. STR and STR2 evolved from duplication in land plants. B) Expression of the *Lunularia cruciate* orthologs, *LcSTR* and *LcSTR2*, is up-regulated during mycorrhization.

Figure S14. Maximum-likelihood tree of the Glycerol-3-phosphate acyltransferases identified in the extended dataset.

Figure S15. A) Maximum-likelihood phylogenetic tree of RAM2 extracted from the GPAT tree on the left. High-resolution image of the GPAT tree is available in Figure S14. RAM2 originates in

land-plants. Two paralogs are present in liverworts. B) Expression of both paralogs is up-regulated during mycorrhization in the liverwort *Lunularia cruciata.* C) RAM2 is composed by two domains, a haloacid dehydrogenase domain and an acetyltransferase domain. These two types of domains are present in other eukaryotes, including chlorophytes and charophytes, but their combination is unique to GPAT.

Figure S16. A) Maximum-likelihood tree of VAPYRIN. VAPYRIN appeared in land plants and is conserved as a single copy gene. B) VAPYRIN is composed by two domains: a motile-sperm domain combined with Ankyrin repeates. These two types of domains are present in other eukaryotes, including chlorophytes and charophytes, but their combination is unique to VAPYRIN.

Figure S17. Maximum-likelihood tree of the H^+-ATPase identified in the extended dataset.

Figure S18. Maximum-likelihood tree of the Phosphate transporters identified in the extended dataset.

Figure S19. Maximum-likelihood tree of the Phosphate transporter of the PT4 and LcPT clades. High-resolution image of the phosphate transporter tree is available in Figure S18. B) Expression of *LcPT*, from *Lunularia cruciata* is up-regulated during mycorrhization (here contig_26970, the other contig spanning *LcPT*, contig_49319, shows a 406-fold up-regulation).

Figure S20. Drops corresponding to 500, 200 and 100 ng of purified proteins were plotted on a membrane and incubated in presence of calcium and biotinylated calmodulin or with biotinylated calmodulin only (see Appendix S1 for details). *Left:* blot revealed with Poncea S staining. *Right:* gel revealed using streptavidin-conjugated horseradish peroxidase and ECL western blotting reagent. For each protein at least three assays have been conducted including two with all the proteins on the same membrane. One of these experiments is presented here. In absence of calcium no binding was detected.

Figure S21. A) Transgenic roots of A17 (WT) or *ccamk-1* mutant transformed with the constructs used for trans-complementation assays. These constructs contain a constitutively expressed red fluorescent protein (DSRED) as a transformation marker. This marker was used to select transgenic roots for all the experiments. B) RNA samples were extracted from collected transgenic roots and the expression of the transgenes tested by RT-PCR. In parallel, expression of *DSRED* was confirmed. Expression of the transgenes and *DSRED* was confirmed on a total of four plants per construct coming from two independent experiments. C) Primers used to validate the expression of the transgenes and *DSRED*.

Dataset S1. Extended dataset.

Dataset S2. *Lunularia cruciata* genes up-regulated upon colonization by *Rhizophagus irregularis*.

Dataset S3. Sequences used to generate the phylogenetic trees.

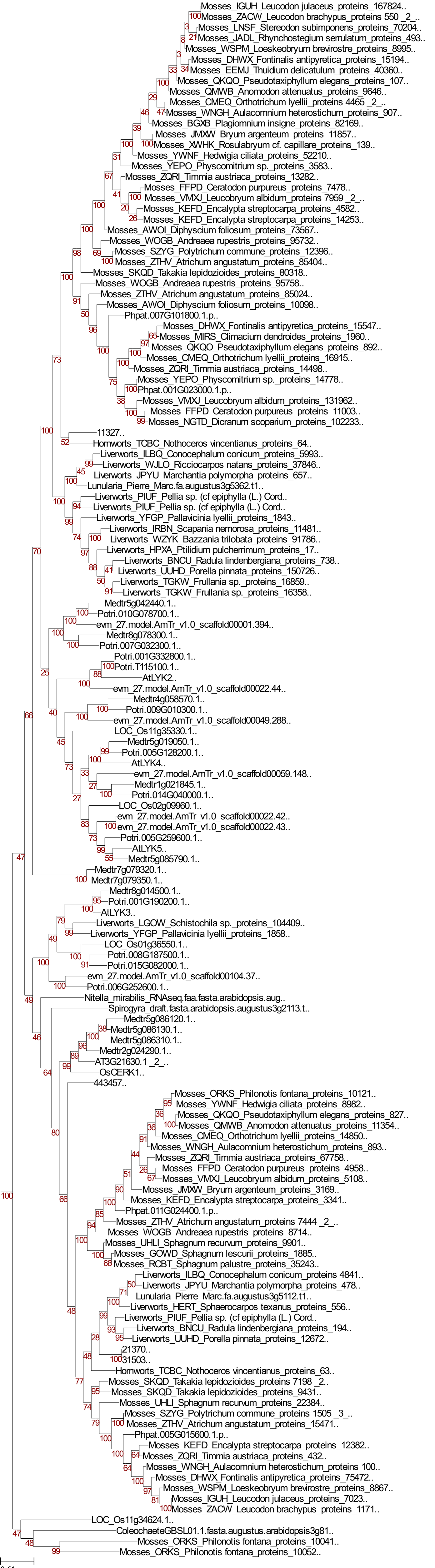
Mosses_IGUH_Leucodon julaceus_proteins_167824..
Mosses_ZACW_Leucodon brachypus_proteins 550 _2_..
Mosses_LNSF_Stereodon subimponens_proteins_70204..
Mosses_JADL_Rhynchostegium serrulatum_proteins_493..
Mosses_WSPM_Loeskeobryum brevirostre_proteins_8995..
Mosses_DHWX_Fontinalis antipyretica_proteins_15194..
Mosses_EEMJ_Thuidium delicatulum_proteins_40360..
Mosses_QKQO_Pseudotaxiphyllum elegans_proteins_107..
Mosses_QMWB_Anomodon attenuatus_proteins_9646..
Mosses_CMEQ_Orthotrichum lyellii_proteins 4465 _2_..
Mosses_WNGH_Aulacomnium heterostichum_proteins_907..
Mosses_BGXB_Plagiomnium insigne_proteins_82169..
Mosses_JMXW_Bryum argenteum_proteins_11857..
Mosses_XWHK_Rosulabryum cf. capillare_proteins_139..
Mosses_YWNF_Hedwigia ciliata_proteins_52210..
Mosses_YEPO_Physcomitrium sp._proteins_3583..
Mosses_ZQRI_Timmia austriaca_proteins_13282..
Mosses_FFPD_Ceratodon purpureus_proteins_7478..
Mosses_VMXJ_Leucobryum albidum_proteins 7959 _2_..
Mosses_KEFD_Encalypta streptocarpa_proteins_4582..
Mosses_KEFD_Encalypta streptocarpa_proteins_14253..
Mosses_AWOI_Diphyscium foliosum_proteins_73567..
Mosses_WOGB_Andreaea rupestris_proteins_95732..
Mosses_SZYG_Polytrichum commune_proteins_12396..
Mosses_ZTHV_Atrichum angustatum_proteins_85404..
Mosses_SKQD_Takakia lepidozioides_proteins_80318..
Mosses_WOGB_Andreaea rupestris_proteins_95758..
Mosses_ZTHV_Atrichum angustatum_proteins_85024..
Mosses_AWOI_Diphyscium foliosum_proteins_10098..
Phpat.007G101800.1.p..
Mosses_DHWX_Fontinalis antipyretica_proteins_15547..
Mosses_MIRS_Climacium dendroides_proteins_1960..
Mosses_QKQO_Pseudotaxiphyllum elegans_proteins_892..
Mosses_CMEQ_Orthotrichum lyellii_proteins_16915..
Mosses_ZQRI_Timmia austriaca_proteins_14498..
Mosses_YEPO_Physcomitrium sp._proteins_14778..
Phpat.001G023000.1.p..
Mosses_VMXJ_Leucobryum albidum_proteins_131962..
Mosses_FFPD_Ceratodon purpureus_proteins_11003..
Mosses_NGTD_Dicranum scoparium_proteins_102233..
11327..
Hornworts_TCBC_Nothoceros vincentianus_proteins_64..
Liverworts_ILBQ_Conocephalum conicum_proteins_5993..
Liverworts_WJLO_Ricciocarpos natans_proteins_37846..
Liverworts_JPYU_Marchantia polymorpha_proteins_657..
Lunularia_Pierre_Marc.fa.augustus3g5362.t1..
Liverworts_PIUF_Pellia sp. (cf epiphylla (L.) Cord..
Liverworts_PIUF_Pellia sp. (cf epiphylla (L.) Cord..
Liverworts_YFGP_Pallavicinia lyellii_proteins_1843..
Liverworts_IRBN_Scapania nemorosa_proteins_11481..
Liverworts_WZYK_Bazzania trilobata_proteins_91786..
Liverworts_HPXA_Ptilidium pulcherrimum_proteins_17..
Liverworts_BNCU_Radula lindenbergiana_proteins_738..
Liverworts_UUHD_Porella pinnata_proteins_150726..
Liverworts_TGKW_Frullania sp._proteins_16859..
Liverworts_TGKW_Frullania sp._proteins_16358..
Medtr5g042440.1..
Potri.010G078700.1..
evm_27.model.AmTr_v1.0_scaffold00001.394..
Medtr8g078300.1..
Potri.007G032300.1..
Potri.001G332800.1..
Potri.T115100.1..
AtLYK2..
evm_27.model.AmTr_v1.0_scaffold00022.44..
Medtr4g058570.1..
Potri.009G010300.1..
evm_27.model.AmTr_v1.0_scaffold00049.288..
LOC_Os11g35330.1..
Medtr5g019050.1..
Potri.005G128200.1..
AtLYK4..
evm_27.model.AmTr_v1.0_scaffold00059.148..
Medtr1g021845.1..
Potri.014G040000.1..
LOC_Os02g09960.1..
evm_27.model.AmTr_v1.0_scaffold00022.42..
evm_27.model.AmTr_v1.0_scaffold00022.43..
Potri.005G259600.1..
AtLYK5..
Medtr5g085790.1..
Medtr7g079320.1..
Medtr7g079350.1..
Medtr8g014500.1..
Potri.001G190200.1..
AtLYK3..
Liverworts_LGOW_Schistochila sp._proteins_104409..
Liverworts_YFGP_Pallavicinia lyellii_proteins_1858..
LOC_Os01g36550.1..
Potri.008G187500.1..
Potri.015G082000.1..
evm_27.model.AmTr_v1.0_scaffold00104.37..
Potri.006G252600.1..
Nitella_mirabilis_RNAseq.faa.fasta.arabidopsis.aug..
Spirogyra_draft.fasta.arabidopsis.augustus3g2113.t..
Medtr5g086120.1..
Medtr5g086130.1..
Medtr5g086310.1..
Medtr2g024290.1..
AT3G21630.1 _2_..
OsCERK1..
443457..
Mosses_ORKS_Philonotis fontana_proteins_10121..
Mosses_YWNF_Hedwigia ciliata_proteins_8982..
Mosses_QKQO_Pseudotaxiphyllum elegans_proteins_827..
Mosses_QMWB_Anomodon attenuatus_proteins_11354..
Mosses_CMEQ_Orthotrichum lyellii_proteins_14850..
Mosses_WNGH_Aulacomnium heterostichum_proteins_893..
Mosses_ZQRI_Timmia austriaca_proteins_67758..
Mosses_FFPD_Ceratodon purpureus_proteins_4958..
Mosses_VMXJ_Leucobryum albidum_proteins_5108..
Mosses_JMXW_Bryum argenteum_proteins_3169..
Mosses_KEFD_Encalypta streptocarpa_proteins_3341..
Phpat.011G024400.1.p..
Mosses_ZTHV_Atrichum angustatum_proteins 7444 _2_..
Mosses_WOGB_Andreaea rupestris_proteins_8714..
Mosses_UHLI_Sphagnum recurvum_proteins_9901..
Mosses_GOWD_Sphagnum lescurii_proteins_1885..
Mosses_RCBT_Sphagnum palustre_proteins_35243..
Liverworts_ILBQ_Conocephalum conicum_proteins 4841..
Liverworts_JPYU_Marchantia polymorpha_proteins_478..
Lunularia_Pierre_Marc.fa.augustus3g5112.t1..
Liverworts_HERT_Sphaerocarpos texanus_proteins_556..
Liverworts_PIUF_Pellia sp. (cf epiphylla (L.) Cord..
Liverworts_BNCU_Radula lindenbergiana_proteins_194..
Liverworts_UUHD_Porella pinnata_proteins_12672..
21370..
31503..
Hornworts_TCBC_Nothoceros vincentianus_proteins_63..
Mosses_SKQD_Takakia lepidozioides_proteins 7198 _2..
Mosses_SKQD_Takakia lepidozioides_proteins_9431..
Mosses_UHLI_Sphagnum recurvum_proteins_22384..
Mosses_SZYG_Polytrichum commune_proteins 1505 _3_..
Mosses_ZTHV_Atrichum angustatum_proteins_15471..
Phpat.005G015600.1.p..
Mosses_KEFD_Encalypta streptocarpa_proteins_12382..
Mosses_ZQRI_Timmia austriaca_proteins_432..
Mosses_WNGH_Aulacomnium heterostichum_proteins 100..
Mosses_DHWX_Fontinalis antipyretica_proteins_75472..
Mosses_WSPM_Loeskeobryum brevirostre_proteins_8867..
Mosses_IGUH_Leucodon julaceus_proteins_7023..
Mosses_ZACW_Leucodon brachypus_proteins_1171..
LOC_Os11g34624.1..
ColeochaeteGBSL01.1.fasta.augustus.arabidopsis3g81..
Mosses_ORKS_Philonotis fontana_proteins_10041..
Mosses_ORKS_Philonotis fontana_proteins_10052..
0.61


LOC_Os04g09961.2
Os04t0209600-01
LOC_Os04g09970.1
Os04t0210100-01
Os04t0210100-02
PPrun.01G04400.1
Pp1s1_1V6.1
Pp1s1_1V6.2
Pp1s1_1V6.3
Pp1s1_1V6.4
Pp1s1_1V6.5
Pp1s1_1V6.6
Pp1s1_1V6.7
Pp1s1_1V6.8
Pp1s1_1V6.9
Pp1s1_1V6.10
Pp1s1_1V6.11
Pp1s1_1V6.12
Pp1s1_1V6.13
Pp1s1_1V6.14
Pp1s1_1V6.15
Pp1s1_1V6.16
Pp1s1_1V6.17
Pp1s1_1V6.18
Pp1s1_1V6.19
Pp1s1_1V6.20
Pp1s1_1V6.21
Pp1s1_1V6.22
Pp1s1_1V6.23
Pp1s1_1V6.24
Pp1s1_1V6.25
Pp1s1_1V6.26
Pp1s1_1V6.27
Pp1s1_1V6.28
Pp1s1_1V6.29
Pp1s1_1V6.30
Pp1s1_1V6.31
Pp1s1_1V6.32
Pp1s1_1V6.33
Pp1s1_1V6.34
Pp1s1_1V6.35
Pp1s1_1V6.36
Pp1s1_1V6.37
Pp1s1_1V6.38
Pp1s1_1V6.39
Pp1s1_1V6.40
Pp1s1_1V6.41
Pp1s1_1V6.42
Pp1s1_1V6.43
Pp1s1_1V6.44
Pp1s1_1V6.45
Pp1s1_1V6.46
Pp1s1_1V6.47
Pp1s1_1V6.48
Pp1s1_1V6.49

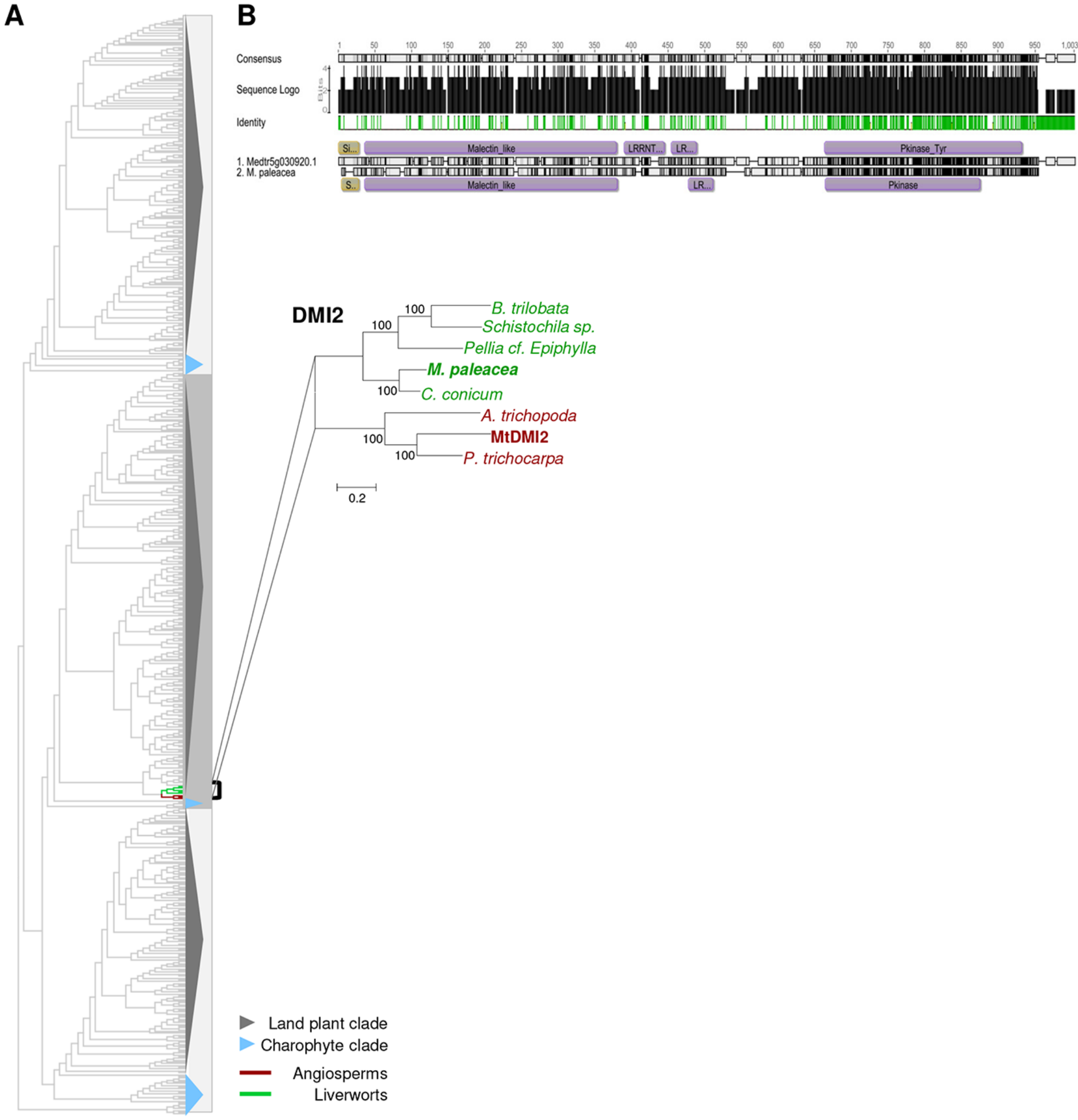
A
B
Consensus
Sequence Logo
Identity
Bits
1 50 100 150 200 250 300 350 400 450 500 550 600 650 700 750 800 850 900 950 1,003
Si...
Malectin_like
LRRNT...
LR...
Pkinase_Tyr
1. Medtr5g030920.1
2. M. paleacea
S..
Malectin_like
LR...
Pkinase
DMI2
100
100
100
100
100
B. trilobata
Schistochila sp.
Pellia cf. Epiphylla
M. paleacea
C. conicum
A. trichopoda
MtDMI2
P. trichocarpa
0.2
Land plant clade
Charophyte clade
Angiosperms
Liverworts

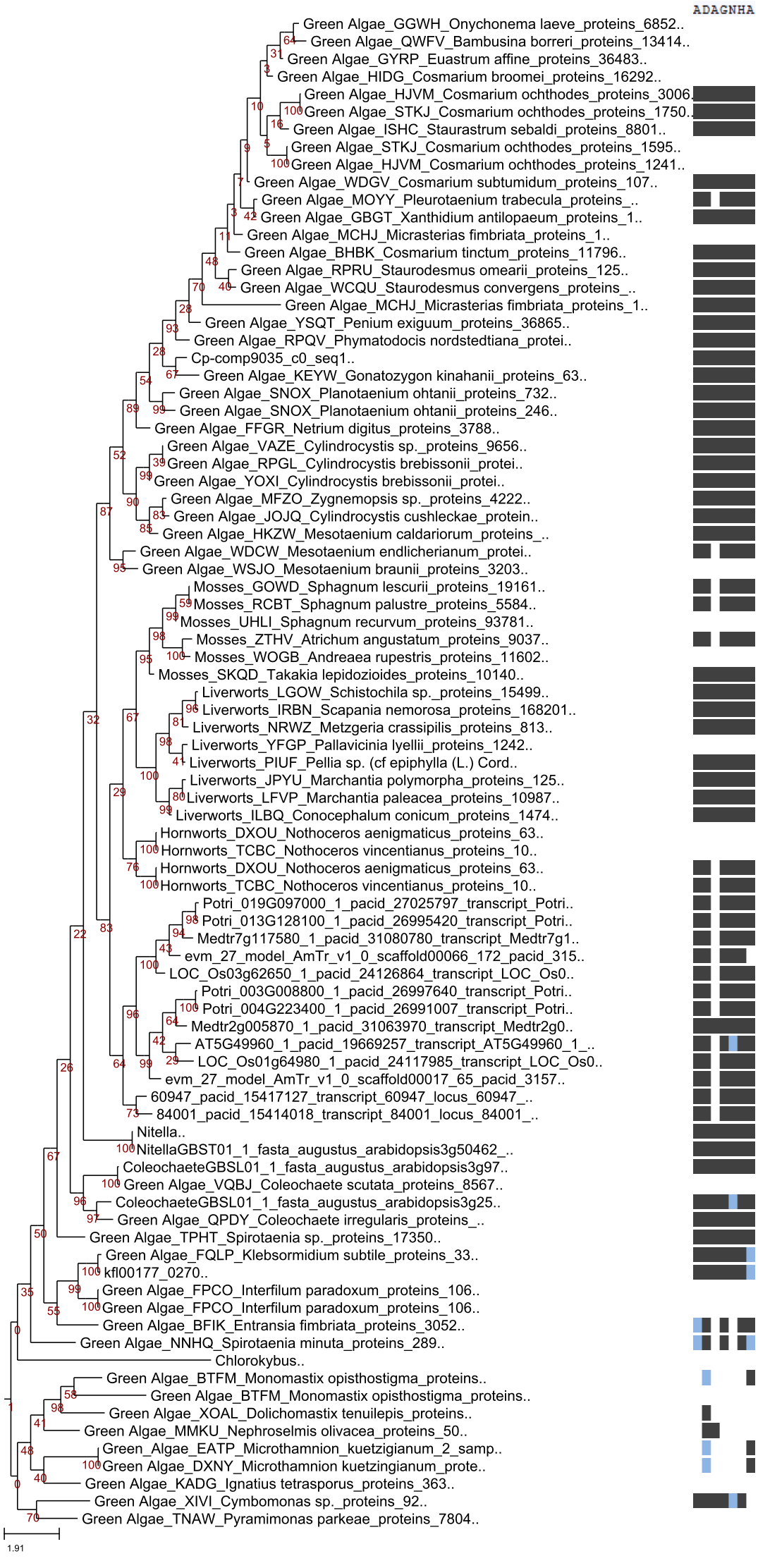
ADAGNHA
Green Algae_GGWH_Onychonema laeve_proteins_6852..
Green Algae_QWFV_Bambusina borreri_proteins_13414..
Green Algae_GYRP_Euastrum affine_proteins_36483..
Green Algae_HIDG_Cosmarium broomei_proteins_16292..
Green Algae_HJVM_Cosmarium ochthodes_proteins_3006..
Green Algae_STKJ_Cosmarium ochthodes_proteins_1750..
Green Algae_ISHC_Staurastrum sebaldi_proteins_8801..
Green Algae_STKJ_Cosmarium ochthodes_proteins_1595..
Green Algae_HJVM_Cosmarium ochthodes_proteins_1241..
Green Algae_WDGV_Cosmarium subtumidum_proteins_107..
Green Algae_MOYY_Pleurotaenium trabecula_proteins_..
Green Algae_GBGT_Xanthidium antilopaeum_proteins_1..
Green Algae_MCHJ_Micrasterias fimbriata_proteins_1..
Green Algae_BHBK_Cosmarium tinctum_proteins_11796..
Green Algae_RPRU_Staurodesmus omearii_proteins_125..
Green Algae_WCQU_Staurodesmus convergens_proteins_..
Green Algae_MCHJ_Micrasterias fimbriata_proteins_1..
Green Algae_YSQT_Penium exiguum_proteins_36865..
Green Algae_RPQV_Phymatodocis nordstedtiana_protei..
Cp-comp9035_c0_seq1..
Green Algae_KEYW_Gonatozygon kinahanii_proteins_63..
Green Algae_SNOX_Planotaenium ohtanii_proteins_732..
Green Algae_SNOX_Planotaenium ohtanii_proteins_246..
Green Algae_FFGR_Netrium digitus_proteins_3788..
Green Algae_VAZE_Cylindrocystis sp._proteins_9656..
Green Algae_RPGL_Cylindrocystis brebissonii_protei..
Green Algae_YOXI_Cylindrocystis brebissonii_protei..
Green Algae_MFZO_Zygnemopsis sp._proteins_4222..
Green Algae_JOJQ_Cylindrocystis cushleckae_protein..
Green Algae_HKZW_Mesotaenium caldariorum_proteins_..
Green Algae_WDCW_Mesotaenium endlicherianum_protei..
Green Algae_WSJO_Mesotaenium braunii_proteins_3203..
Mosses_GOWD_Sphagnum lescurii_proteins_19161..
Mosses_RCBT_Sphagnum palustre_proteins_5584..
Mosses_UHLI_Sphagnum recurvum_proteins_93781..
Mosses_ZTHV_Atrichum angustatum_proteins_9037..
Mosses_WOGB_Andreaea rupestris_proteins_11602..
Mosses_SKQD_Takakia lepidozioides_proteins_10140..
Liverworts_LGOW_Schistochila sp._proteins_15499..
Liverworts_IRBN_Scapania nemorosa_proteins_168201..
Liverworts_NRWZ_Metzgeria crassipilis_proteins_813..
Liverworts_YFGP_Pallavicinia lyellii_proteins_1242..
Liverworts_PIUF_Pellia sp. (cf epiphylla (L.) Cord..
Liverworts_JPYU_Marchantia polymorpha_proteins_125..
Liverworts_LFVP_Marchantia paleacea_proteins_10987..
Liverworts_ILBQ_Conocephalum conicum_proteins_1474..
Hornworts_DXOU_Nothoceros aenigmaticus_proteins_63..
Hornworts_TCBC_Nothoceros vincentianus_proteins_10..
Hornworts_DXOU_Nothoceros aenigmaticus_proteins_63..
Hornworts_TCBC_Nothoceros vincentianus_proteins_10..
Potri_019G097000_1_pacid_27025797_transcript_Potri..
Potri_013G128100_1_pacid_26995420_transcript_Potri..
Medtr7g117580_1_pacid_31080780_transcript_Medtr7g1..
evm_27_model_AmTr_v1_0_scaffold00066_172_pacid_315..
LOC_Os03g62650_1_pacid_24126864_transcript_LOC_Os0..
Potri_003G008800_1_pacid_26997640_transcript_Potri..
Potri_004G223400_1_pacid_26991007_transcript_Potri..
Medtr2g005870_1_pacid_31063970_transcript_Medtr2g0..
AT5G49960_1_pacid_19669257_transcript_AT5G49960_1_..
LOC_Os01g64980_1_pacid_24117985_transcript_LOC_Os0..
evm_27_model_AmTr_v1_0_scaffold00017_65_pacid_3157..
60947_pacid_15417127_transcript_60947_locus_60947_..
84001_pacid_15414018_transcript_84001_locus_84001_..
Nitella..
NitellaGBST01_1_fasta_augustus_arabidopsis3g50462_..
ColeochaeteGBSL01_1_fasta_augustus_arabidopsis3g97..
Green Algae_VQBJ_Coleochaete scutata_proteins_8567..
ColeochaeteGBSL01_1_fasta_augustus_arabidopsis3g25..
Green Algae_QPDY_Coleochaete irregularis_proteins_..
Green Algae_TPHT_Spirotaenia sp._proteins_17350..
Green Algae_FQLP_Klebsormidium subtile_proteins_33..
kfl00177_0270..
Green Algae_FPCO_Interfilum paradoxum_proteins_106..
Green Algae_FPCO_Interfilum paradoxum_proteins_106..
Green Algae_BFIK_Entransia fimbriata_proteins_3052..
Green Algae_NNHQ_Spirotaenia minuta_proteins_289..
Chlorokybus..
Green Algae_BTFM_Monomastix opisthostigma_proteins..
Green Algae_BTFM_Monomastix opisthostigma_proteins..
Green Algae_XOAL_Dolichomastix tenuilepis_proteins..
Green Algae_MMKU_Nephroselmis olivacea_proteins_50..
Green_Algae_EATP_Microthamnion_kuetzigianum_2_samp..
Green Algae_DXNY_Microthamnion kuetzingianum_prote..
Green Algae_KADG_Ignatius tetrasporus_proteins_363..
Green Algae_XIVI_Cymbomonas sp._proteins_92..
Green Algae_TNAW_Pyramimonas parkeae_proteins_7804..
1.91

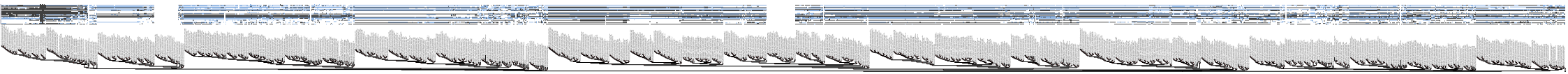

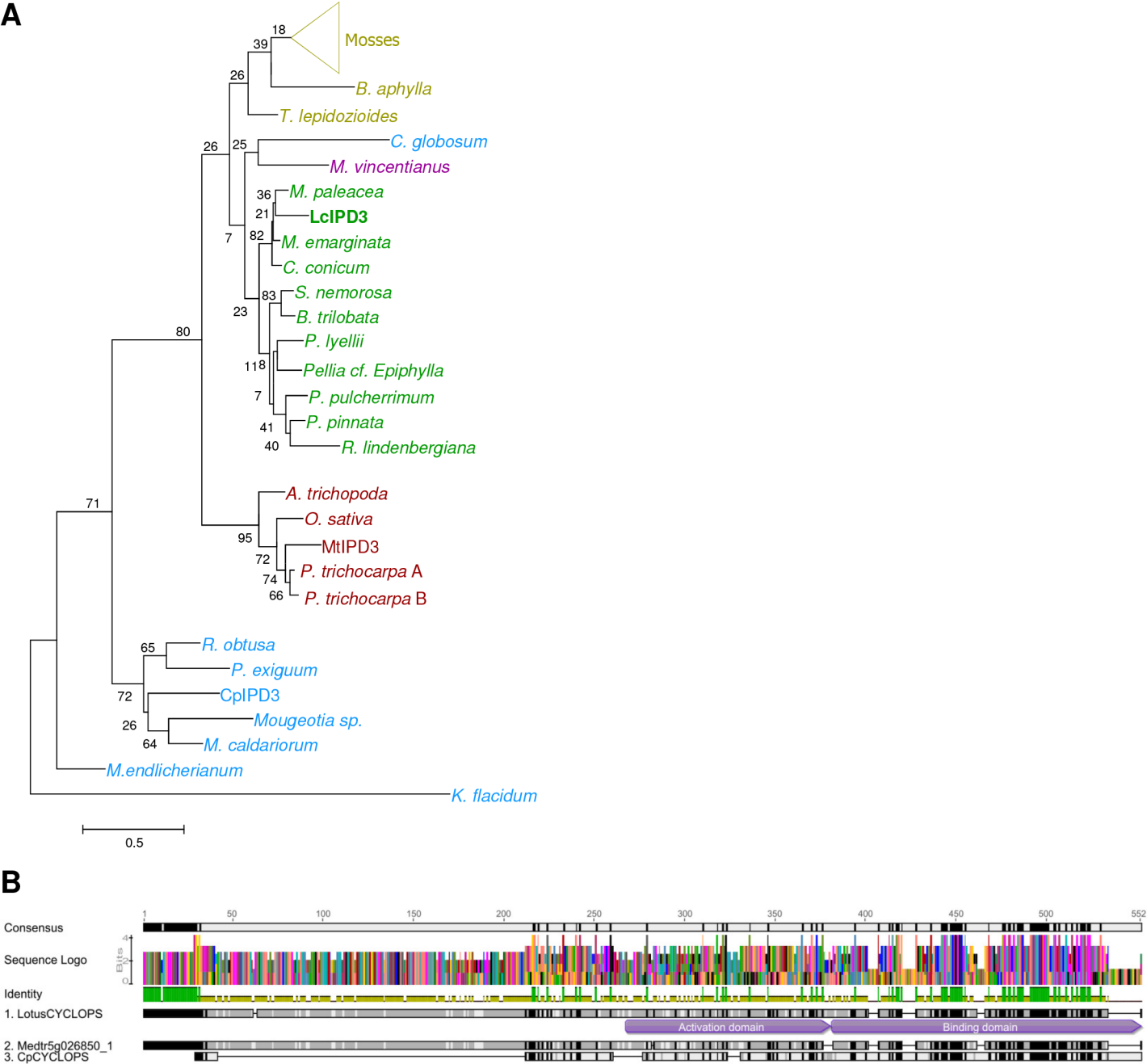
A
Mosses
B. aphylla
T. lepidozioides
C. globosum
M. vincentianus
M. paleacea
LcIPD3
M. emarginata
C. conicum
S. nemorosa
B. trilobata
P. lyellii
Pellia cf. Epiphylla
P. pulcherrimum
P. pinnata
R. lindenbergiana
A. trichopoda
O. sativa
MtIPD3
P. trichocarpa A
P. trichocarpa B
R. obtusa
P. exiguum
CpIPD3
Mougeotia sp.
M. caldariorum
M.endlicherianum
K. flacidum
0.5
B
Consensus
Sequence Logo
Bits
Identity
1. LotusCYCLOPS
Activation domain
Binding domain
2. Medtr5g026850_1
3. CpCYCLOPS

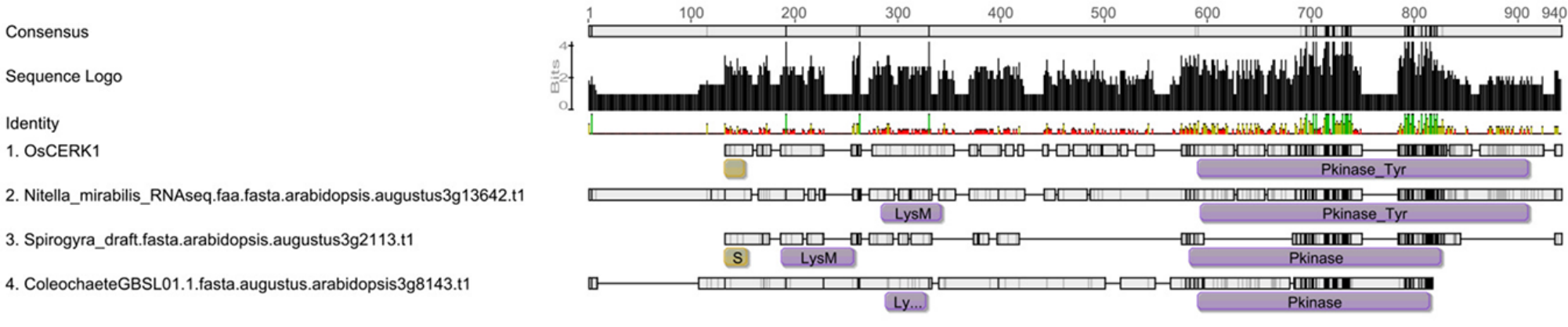
Consensus
Sequence Logo
Identity
1. OsCERK1
2. Nitella_mirabilis_RNAseq.faa.fasta.arabidopsis.augustus3g13642.t1
3. Spirogyra_draft.fasta.arabidopsis.augustus3g2113.t1
4. ColeochaeteGBSL01.1.fasta.augustus.arabidopsis3g8143.t1
1
100
200
300
400
500
600
700
800
900
940
Bits
4
2
0
Pkinase_Tyr
LysM
Pkinase_Tyr
S
LysM
Pkinase
Ly...
Pkinase

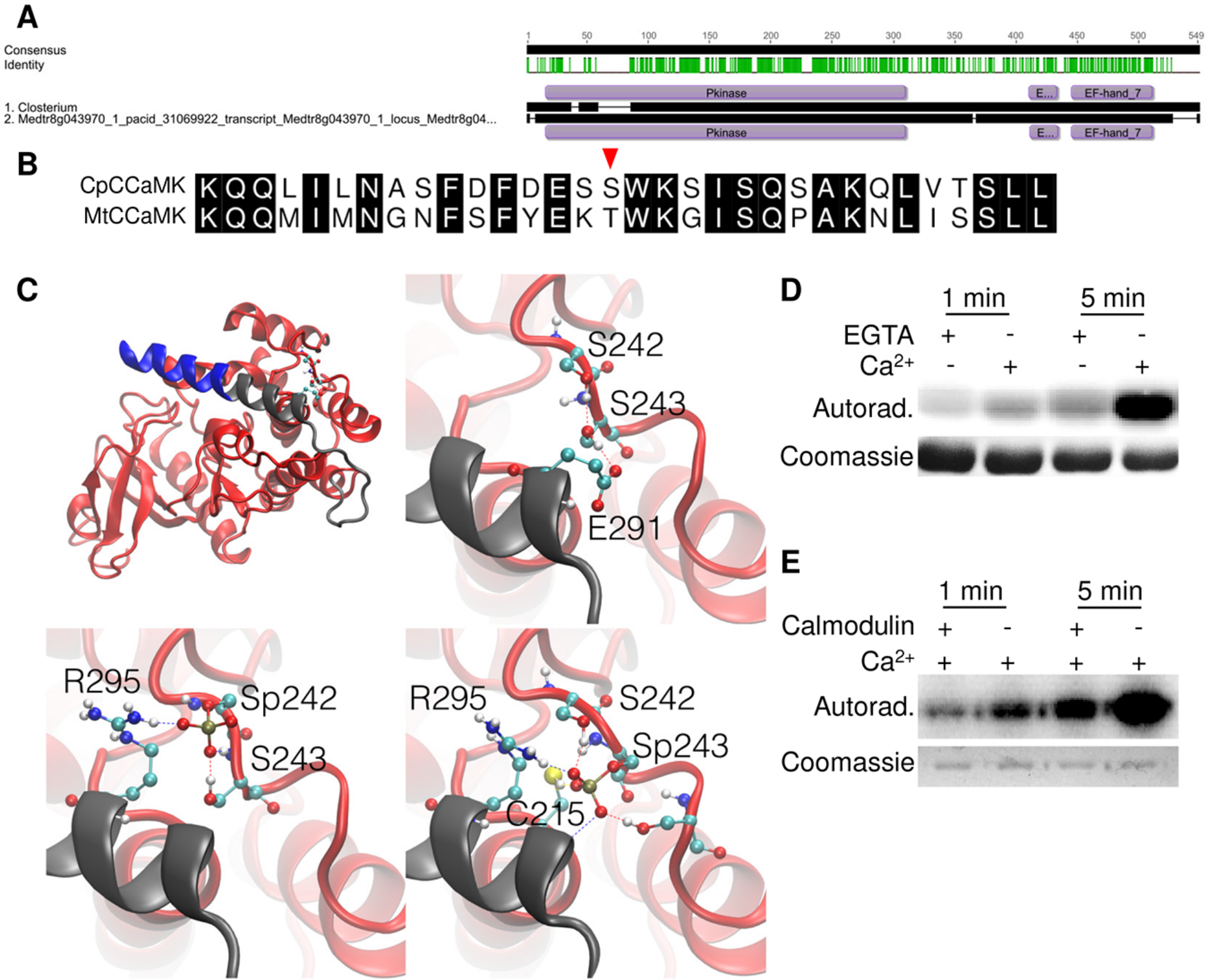
A
Consensus
Identity
1 50 100 150 200 250 300 350 400 450 500 549
Pkinase
E...
EF-hand_7
1. Closterium
2. Medtr8g043970_1_pacid_31069922_transcript_Medtr8g043970_1_locus_Medtr8g04...
Pkinase
E...
EF-hand_7
B
CpCCaMK K Q Q L I L N A S F D F D E S S W K S I S Q S A K Q L V T S L L
MtCCaMK K Q Q M I M N G N F S F Y E K T W K G I S Q P A K N L I S S L L
C
S242
S243
E291
R295
Sp242
S243
R295
S242
Sp243
C215
D
1 min
5 min
EGTA + - + -
Ca2+ - + - +
Autorad.
Coomassie
E
1 min
5 min
Calmodulin + - + -
Ca2+ + + + +
Autorad.
Coomassie

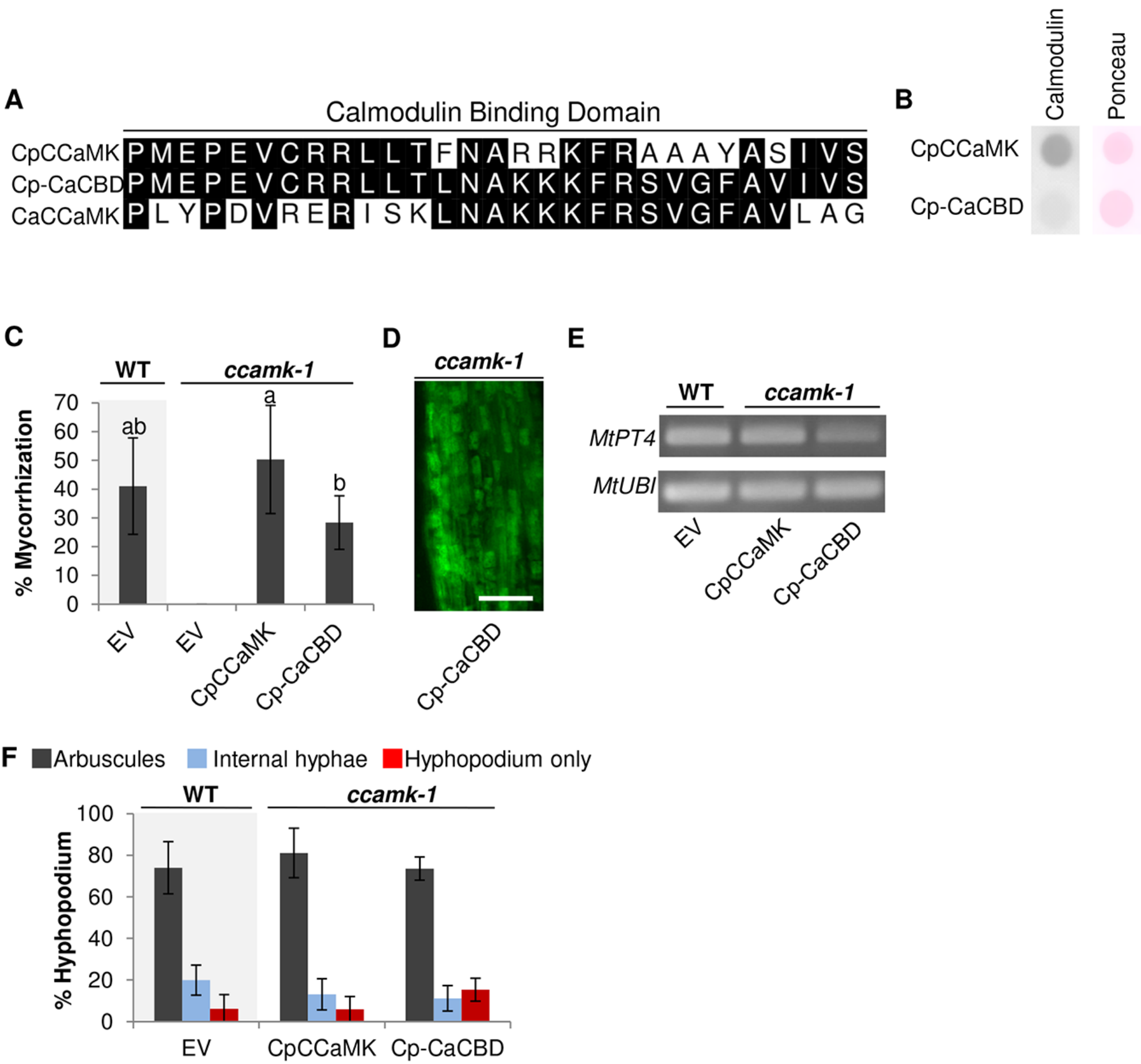
A
Calmodulin Binding Domain
CpCCaMK PMEPEVCRRLLTFNARRKFRAAAAYASIVS
Cp-CaCBD PMEPEVCRRLLTLNAKKKFRSVGFAVIVS
CaCCaMK PLYPDVRERISKLNAKKKFRSVGFAVLAG
B
Calmodulin
Ponceau
CpCCaMK
Cp-CaCBD
C
WT
ccamk-1
% Mycorrhization
70
60
50
40
30
20
10
0
ab
a
b
EV
EV
CpCCaMK
Cp-CaCBD
D
ccamk-1
Cp-CaCBD
E
WT
ccamk-1
MtPT4
MtUBI
EV
CpCCaMK
Cp-CaCBD
F
Arbuscules
Internal hyphae
Hyphopodium only
WT
ccamk-1
% Hyphopodium
100
80
60
40
20
0
EV
CpCCaMK
Cp-CaCBD

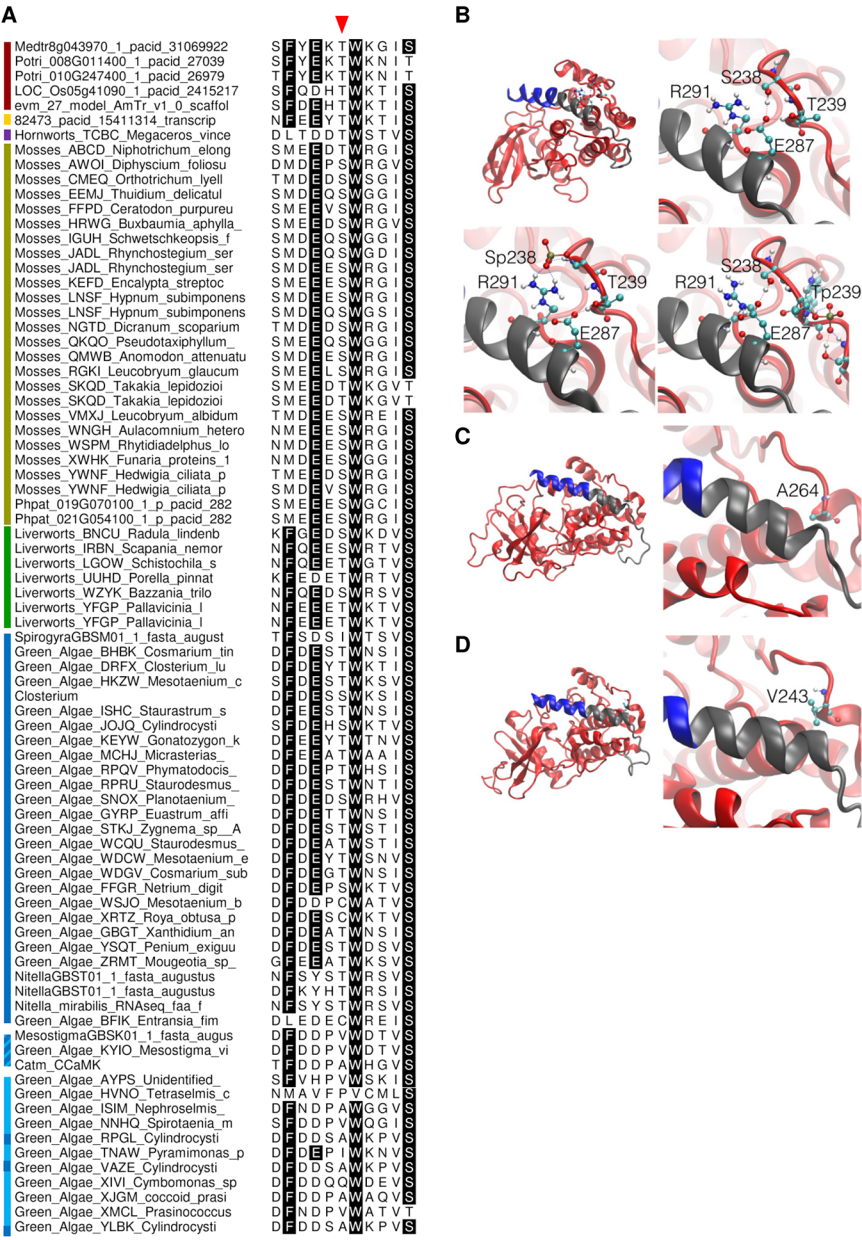
A
Medtr8g043970_1_pacid_31069922
Potri_008G011400_1_pacid_27039
Potri_010G247400_1_pacid_26979
LOC_Os05g41090_1_pacid_2415217
evm_27_model_AmTr_v1_0_scaffol
82473_pacid_15411314_transcrip
Hornworts_TCBC_Megaceros_vince
Mosses_ABCD_Niphotrichum_elong
Mosses_AWOI_Diphyscium_foliosu
Mosses_CMEQ_Orthotrichum_lyell
Mosses_EEMJ_Thuidium_delicatul
Mosses_FFPD_Ceratodon_purpureu
Mosses_HRWG_Buxbaumia_aphylla_
Mosses_IGUH_Schwetschkeopsis_f
Mosses_JADL_Rhynchostegium_ser
Mosses_JADL_Rhynchostegium_ser
Mosses_KEFD_Encalypta_streptoc
Mosses_LNSF_Hypnum_subimponens
Mosses_LNSF_Hypnum_subimponens
Mosses_NGTD_Dicranum_scoparium
Mosses_QKQO_Pseudotaxiphyllum_
Mosses_QMWB_Anomodon_attenuatu
Mosses_RGKI_Leucobryum_glaucum
Mosses_SKQD_Takakia_lepidozioi
Mosses_SKQD_Takakia_lepidozioi
Mosses_VMXJ_Leucobryum_albidum
Mosses_WNGH_Aulacomnium_hetero
Mosses_WSPM_Rhytidiadelphus_lo
Mosses_XWHK_Funaria_proteins_1
Mosses_YWNF_Hedwigia_ciliata_p
Mosses_YWNF_Hedwigia_ciliata_p
Phpat_019G070100_1_p_pacid_282
Phpat_021G054100_1_p_pacid_282
Liverworts_BNCU_Radula_lindenb
Liverworts_IRBN_Scapania_nemor
Liverworts_LGOW_Schistochila_s
Liverworts_UUHD_Porella_pinnat
Liverworts_WZYK_Bazzania_trilo
Liverworts_YFGP_Pallavicinia_l
Liverworts_YFGP_Pallavicinia_l
SpirogyraGBSM01_1_fasta_august
Green_Algae_BHBK_Cosmarium_tin
Green_Algae_DRFX_Closterium_lu
Green_Algae_HKZW_Mesotaenium_c
Closterium
Green_Algae_ISHC_Staurastrum_s
Green_Algae_JOJQ_Cylindrocysti
Green_Algae_KEYW_Gonatozygon_k
Green_Algae_MCHJ_Micrasterias_
Green_Algae_RPQV_Phymatodocis_
Green_Algae_RPRU_Staurodesmus_
Green_Algae_SNOX_Planotaenium_
Green_Algae_GYRP_Euastrum_affi
Green_Algae_STKJ_Zygnema_sp__A
Green_Algae_WCQU_Staurodesmus_
Green_Algae_WDCW_Mesotaenium_e
Green_Algae_WDGV_Cosmarium_sub
Green_Algae_FFGR_Netrium_digit
Green_Algae_WSJO_Mesotaenium_b
Green_Algae_XRTZ_Roya_obtusa_p
Green_Algae_GBGT_Xanthidium_an
Green_Algae_YSQT_Penium_exiguu
Green_Algae_ZRMT_Mougeotia_sp_
NitellaGBST01_1_fasta_augustus
NitellaGBST01_1_fasta_augustus
Nitella_mirabilis_RNAseq_faa_f
Green_Algae_BFIK_Entransia_fim
MesostigmaGBSK01_1_fasta_augus
Green_Algae_KYIO_Mesostigma_vi
Catm_CCaMK
Green_Algae_AYPS_Unidentified_
Green_Algae_HVNO_Tetraselmis_c
Green_Algae_ISIM_Nephroselmis_
Green_Algae_NNHQ_Spirotaenia_m
Green_Algae_RPGL_Cylindrocysti
Green_Algae_TNAW_Pyramimonas_p
Green_Algae_VAZE_Cylindrocysti
Green_Algae_XIVI_Cymbomonas_sp
Green_Algae_XJGM_coccoid_prasi
Green_Algae_XMCL_Prasinococcus
Green_Algae_YLBK_Cylindrocysti
B
S238
R291
T239
E287
Sp238
R291
T239
E287
S238
R291
Tp239
E287
C
A264
D
V243

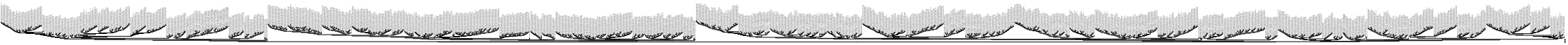

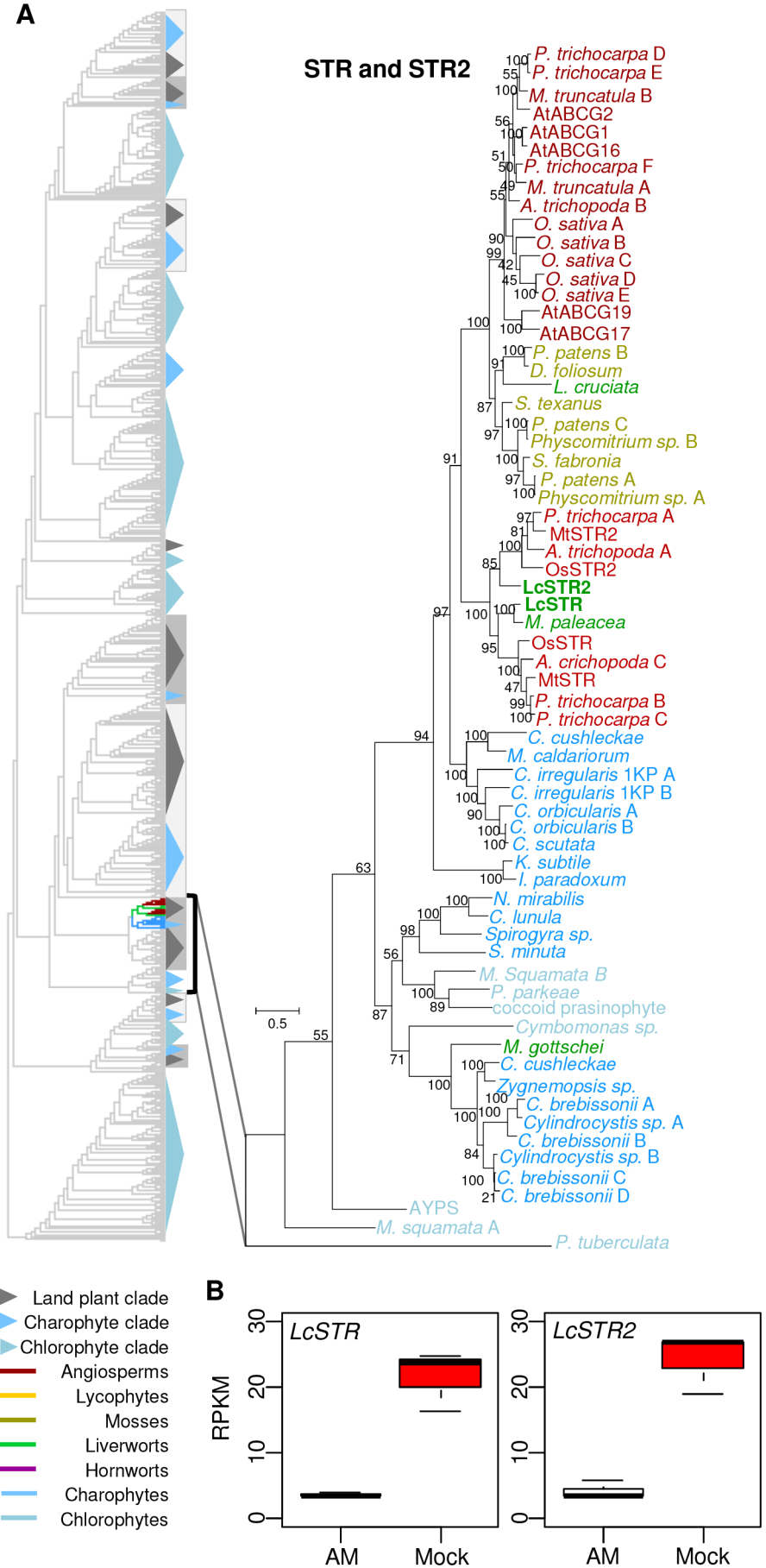
A
STR and STR2
P. trichocarpa D
P. trichocarpa E
M. truncatula B
AtABCG2
AtABCG1
AtABCG16
P. trichocarpa F
M. truncatula A
A. trichopoda B
O. sativa A
O. sativa B
O. sativa C
O. sativa D
O. sativa E
AtABCG19
AtABCG17
P. patens B
D. foliosum
L. cruciata
S. texanus
P. patens C
Physcomitrium sp. B
S. fabronia
P. patens A
Physcomitrium sp. A
P. trichocarpa A
MtSTR2
A. trichopoda A
OsSTR2
LcSTR2
LcSTR
M. paleacea
OsSTR
A. crichopoda C
MtSTR
P. trichocarpa B
P. trichocarpa C
C. cushleckae
M. caldariorum
C. irregularis 1KP A
C. irregularis 1KP B
C. orbicularis A
C. orbicularis B
C. scutata
K. subtile
I. paradoxum
N. mirabilis
C. lunula
Spirogyra sp.
S. minuta
M. Squamata B
P. parkeae
coccoid prasinophyte
Cymbomonas sp.
M. gottschei
C. cushleckae
Zygnemopsis sp.
C. brebissonii A
Cylindrocystis sp. A
C. brebissonii B
Cylindrocystis sp. B
C. brebissonii C
C. brebissonii D
AYPS
M. squamata A
P. tuberculata
0.5
Land plant clade
Charophyte clade
Chlorophyte clade
Angiosperms
Lycophytes
Mosses
Liverworts
Hornworts
Charophytes
Chlorophytes
B
LcSTR
LcSTR2
RPKM
0
10
20
30
AM
Mock

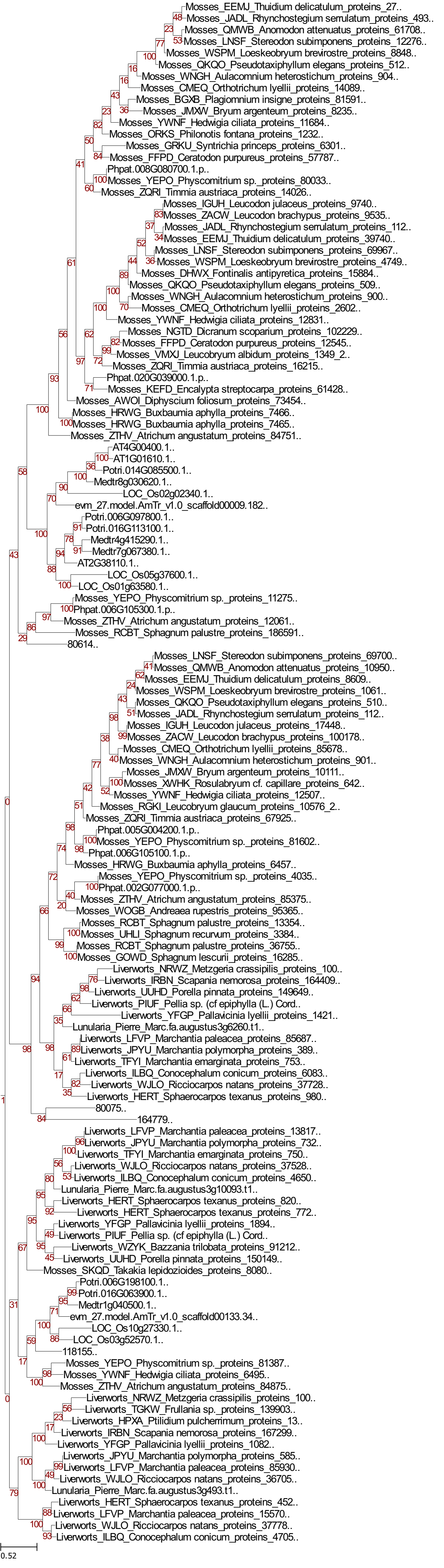
Mosses_EEMJ_Thuidium delicatulum_proteins_27..
Mosses_JADL_Rhynchostegium serrulatum_proteins_493..
Mosses_QMWB_Anomodon attenuatus_proteins_61708..
Mosses_LNSF_Stereodon subimponens_proteins_12276..
Mosses_WSPM_Loeskeobryum brevirostre_proteins_8848..
Mosses_QKQO_Pseudotaxiphyllum elegans_proteins_512..
Mosses_WNGH_Aulacomnium heterostichum_proteins_904..
Mosses_CMEQ_Orthotrichum lyellii_proteins_14089..
Mosses_BGXB_Plagiomnium insigne_proteins_81591..
Mosses_JMXW_Bryum argenteum_proteins_8235..
Mosses_YWNF_Hedwigia ciliata_proteins_11684..
Mosses_ORKS_Philonotis fontana_proteins_1232..
Mosses_GRKU_Syntrichia princeps_proteins_6301..
Mosses_FFPD_Ceratodon purpureus_proteins_57787..
Phpat.008G080700.1.p..
Mosses_YEPO_Physcomitrium sp._proteins_80033..
Mosses_ZQRI_Timmia austriaca_proteins_14026..
Mosses_IGUH_Leucodon julaceus_proteins_9740..
Mosses_ZACW_Leucodon brachypus_proteins_9535..
Mosses_JADL_Rhynchostegium serrulatum_proteins_112..
Mosses_EEMJ_Thuidium delicatulum_proteins_39740..
Mosses_LNSF_Stereodon subimponens_proteins_69967..
Mosses_WSPM_Loeskeobryum brevirostre_proteins_4749..
Mosses_DHWX_Fontinalis antipyretica_proteins_15884..
Mosses_QKQO_Pseudotaxiphyllum elegans_proteins_509..
Mosses_WNGH_Aulacomnium heterostichum_proteins_900..
Mosses_CMEQ_Orthotrichum lyellii_proteins_2602..
Mosses_YWNF_Hedwigia ciliata_proteins_12831..
Mosses_NGTD_Dicranum scoparium_proteins_102229..
Mosses_FFPD_Ceratodon purpureus_proteins_12545..
Mosses_VMXJ_Leucobryum albidum_proteins_1349_2..
Mosses_ZQRI_Timmia austriaca_proteins_16215..
Phpat.020G039000.1.p..
Mosses_KEFD_Encalypta streptocarpa_proteins_61428..
Mosses_AWOI_Diphyscium foliosum_proteins_73454..
Mosses_HRWG_Buxbaumia aphylla_proteins_7466..
Mosses_HRWG_Buxbaumia aphylla_proteins_7465..
Mosses_ZTHV_Atrichum angustatum_proteins_84751..
AT4G00400.1..
AT1G01610.1..
Potri.014G085500.1..
Medtr8g030620.1..
LOC_Os02g02340.1..
evm_27.model.AmTr_v1.0_scaffold00009.182..
Potri.006G097800.1..
Potri.016G113100.1..
Medtr4g415290.1..
Medtr7g067380.1..
AT2G38110.1..
LOC_Os05g37600.1..
LOC_Os01g63580.1..
Mosses_YEPO_Physcomitrium sp._proteins_11275..
Phpat.006G105300.1.p..
Mosses_ZTHV_Atrichum angustatum_proteins_12061..
Mosses_RCBT_Sphagnum palustre_proteins_186591..
80614..
Mosses_LNSF_Stereodon subimponens_proteins_69700..
Mosses_QMWB_Anomodon attenuatus_proteins_10950..
Mosses_EEMJ_Thuidium delicatulum_proteins_8609..
Mosses_WSPM_Loeskeobryum brevirostre_proteins_1061..
Mosses_QKQO_Pseudotaxiphyllum elegans_proteins_510..
Mosses_JADL_Rhynchostegium serrulatum_proteins_112..
Mosses_IGUH_Leucodon julaceus_proteins_17448..
Mosses_ZACW_Leucodon brachypus_proteins_100178..
Mosses_CMEQ_Orthotrichum lyellii_proteins_85678..
Mosses_WNGH_Aulacomnium heterostichum_proteins_901..
Mosses_JMXW_Bryum argenteum_proteins_10111..
Mosses_XWHK_Rosulabryum cf. capillare_proteins_642..
Mosses_YWNF_Hedwigia ciliata_proteins_12507..
Mosses_RGKI_Leucobryum glaucum_proteins_10576_2..
Mosses_ZQRI_Timmia austriaca_proteins_67925..
Phpat.005G004200.1.p..
Mosses_YEPO_Physcomitrium sp._proteins_81602..
Phpat.006G105100.1.p..
Mosses_HRWG_Buxbaumia aphylla_proteins_6457..
Mosses_YEPO_Physcomitrium sp._proteins_4035..
Phpat.002G077000.1.p..
Mosses_ZTHV_Atrichum angustatum_proteins_85375..
Mosses_WOGB_Andreaea rupestris_proteins_95365..
Mosses_RCBT_Sphagnum palustre_proteins_13354..
Mosses_UHLI_Sphagnum recurvum_proteins_3384..
Mosses_RCBT_Sphagnum palustre_proteins_36755..
Mosses_GOWD_Sphagnum lescurii_proteins_16285..
Liverworts_NRWZ_Metzgeria crassipilis_proteins_100..
Liverworts_IRBN_Scapania nemorosa_proteins_164409..
Liverworts_UUHD_Porella pinnata_proteins_149649..
Liverworts_PIUF_Pellia sp. (cf epiphylla (L.) Cord..
Liverworts_YFGP_Pallavicinia lyellii_proteins_1421..
Lunularia_Pierre_Marc.fa.augustus3g6260.t1..
Liverworts_LFVP_Marchantia paleacea_proteins_85687..
Liverworts_JPYU_Marchantia polymorpha_proteins_389..
Liverworts_TFYI_Marchantia emarginata_proteins_753..
Liverworts_ILBQ_Conocephalum conicum_proteins_6083..
Liverworts_WJLO_Ricciocarpos natans_proteins_37728..
Liverworts_HERT_Sphaerocarpos texanus_proteins_980..
80075..
164779..
Liverworts_LFVP_Marchantia paleacea_proteins_13817..
Liverworts_JPYU_Marchantia polymorpha_proteins_732..
Liverworts_TFYI_Marchantia emarginata_proteins_750..
Liverworts_WJLO_Ricciocarpos natans_proteins_37528..
Liverworts_ILBQ_Conocephalum conicum_proteins_4650..
Lunularia_Pierre_Marc.fa.augustus3g10093.t1..
Liverworts_HERT_Sphaerocarpos texanus_proteins_820..
Liverworts_HERT_Sphaerocarpos texanus_proteins_772..
Liverworts_YFGP_Pallavicinia lyellii_proteins_1894..
Liverworts_PIUF_Pellia sp. (cf epiphylla (L.) Cord..
Liverworts_WZYK_Bazzania trilobata_proteins_91212..
Liverworts_UUHD_Porella pinnata_proteins_150149..
Mosses_SKQD_Takakia lepidozioides_proteins_8080..
Potri.006G198100.1..
Potri.016G063900.1..
Medtr1g040500.1..
evm_27.model.AmTr_v1.0_scaffold00133.34..
LOC_Os10g27330.1..
LOC_Os03g52570.1..
118155..
Mosses_YEPO_Physcomitrium sp._proteins_81387..
Mosses_YWNF_Hedwigia ciliata_proteins_6495..
Mosses_ZTHV_Atrichum angustatum_proteins_84875..
Liverworts_NRWZ_Metzgeria crassipilis_proteins_100..
Liverworts_TGKW_Frullania sp._proteins_139903..
Liverworts_HPXA_Ptilidium pulcherrimum_proteins_13..
Liverworts_IRBN_Scapania nemorosa_proteins_167299..
Liverworts_YFGP_Pallavicinia lyellii_proteins_1082..
Liverworts_JPYU_Marchantia polymorpha_proteins_585..
Liverworts_LFVP_Marchantia paleacea_proteins_85930..
Liverworts_WJLO_Ricciocarpos natans_proteins_36705..
Lunularia_Pierre_Marc.fa.augustus3g493.t1..
Liverworts_HERT_Sphaerocarpos texanus_proteins_452..
Liverworts_LFVP_Marchantia paleacea_proteins_15570..
Liverworts_WJLO_Ricciocarpos natans_proteins_37778..
Liverworts_ILBQ_Conocephalum conicum_proteins_4705..
0.52

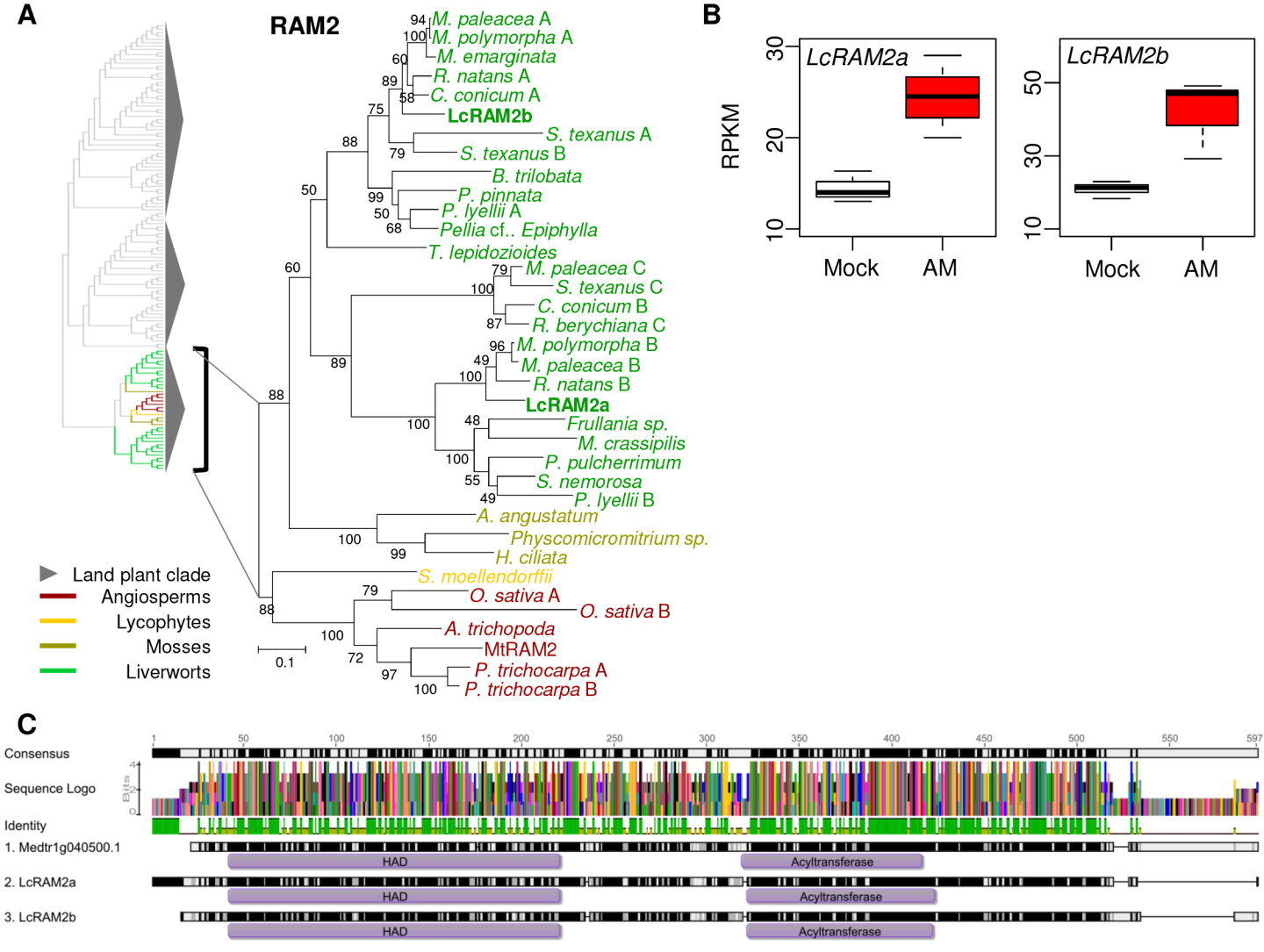
A
RAM2
M. paleacea A
M. polymorpha A
M. emarginata
R. natans A
C. conicum A
LcRAM2b
S. texanus A
S. texanus B
B. trilobata
P. pinnata
P. lyellii A
Pellia cf.. Epiphylla
T. lepidozioides
M. paleacea C
S. texanus C
C. conicum B
R. berychiana C
M. polymorpha B
M. paleacea B
R. natans B
LcRAM2a
Frullania sp.
M. crassipilis
P. pulcherrimum
S. nemorosa
P. lyellii B
A. angustatum
Physcomicromitrium sp.
H. ciliata
S. moellendorffii
O. sativa A
O. sativa B
A. trichopoda
MtRAM2
P. trichocarpa A
P. trichocarpa B
0.1
Land plant clade
Angiosperms
Lycophytes
Mosses
Liverworts
B
RPKM
LcRAM2a
LcRAM2b
Mock
AM
C
Consensus
Sequence Logo
Identity
1. Medtr1g040500.1
2. LcRAM2a
3. LcRAM2b
HAD
Acyltransferase

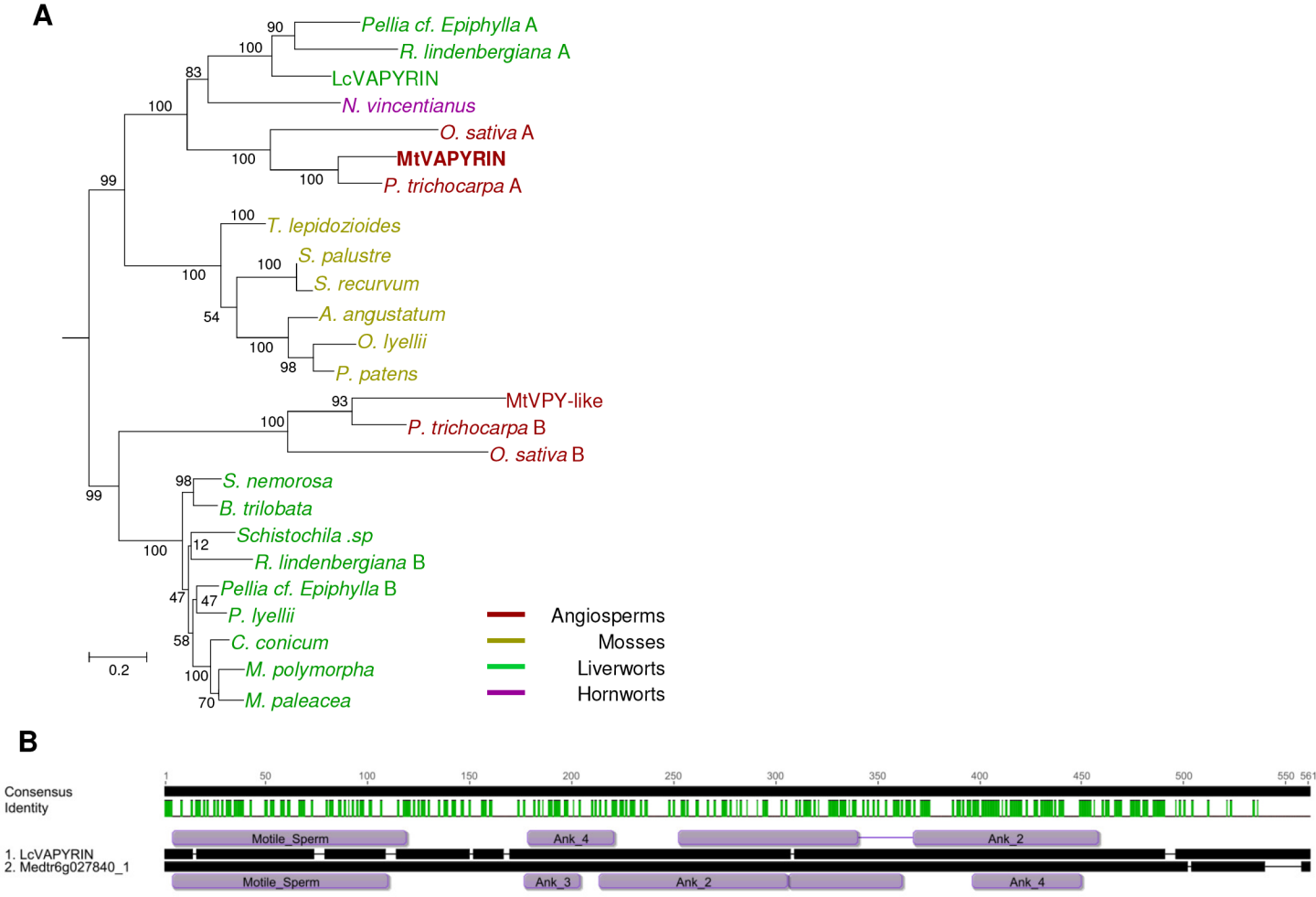
A
Pellia cf. Epiphylla A
R. lindenbergiana A
LcVAPYRIN
N. vincentianus
O. sativa A
MtVAPYRIN
P. trichocarpa A
T. lepidozioides
S. palustre
S. recurvum
A. angustatum
O. lyellii
P. patens
MtVPY-like
P. trichocarpa B
O. sativa B
S. nemorosa
B. trilobata
Schistochila .sp
R. lindenbergiana B
Pellia cf. Epiphylla B
P. lyellii
C. conicum
M. polymorpha
M. paleacea
0.2
Angiosperms
Mosses
Liverworts
Hornworts
B
Consensus
Identity
1. LcVAPYRIN
2. Medtr6g027840_1
Motile_Sperm
Ank_4
Ank_2
Motile_Sperm
Ank_3
Ank_2
Ank_4


0.43


Mosses_MRIS_Climacium dendroides-2001865
Mosses_MRIS_Climacium dendroides-2001866
Mosses_WSPM_Loeskeobryum brevirostre-2008790
Mosses_QKQD_Pseudotaxiphyllum elegans-2000278
Mosses_IGUH_Leucobryum julaceus-2167143
Mosses_ZACW_Leucobrin brachypus-2003733
Mosses_LNSF_Sibirodon sutinoprensis-2007948
Mosses_JADL_Rhynchostegium serrulatum-2048660
Mosses_VBMM_Claopodium rostratum-2003127
Mosses_QNNB_Anomodon attenuatus-2003592
Mosses_TNAJ_Neckera douglasii-2022315
Mosses_YMXJ_Leucobryum albidum-2002650
Mosses_WNGH_Aulacomnium heterostichum-2000695
Mosses_BGXB_Plagiomnium insigne-2006394
Mosses_ORKS_Philonotis fontana-2011510
Mosses_YWNF_Hedwigia ciliata-2051609
Mosses_JMXW_Bryum argenteum-2009271
Mosses_XWHK_Rousiaburyum cf. capillare-2006801
Mosses_XWHK_Rousiaburyum cf. capillare-2006800
Mosses_ABCD_Racomitrium elongatum-2001346
Mosses_RDOO_Racomitrium varium-2014391
Mosses_FFFD_Ceratodon purpureus-2000971
Liverworts_NNQC_mixed species-2158573
Mosses_NCTD_Dicranum scoparium-2003354
Mosses_RGKI_Leucobryum glaucum-2011580
Mosses_YMXJ_Leucobryum albidum-2011961
Mosses_YEPO_Physcomitrium sp.-2081727
Pty XP 001762127.1
Mosses_YEPO_Physcomitrium sp.-2001650
Pty XP 001775821.1
Mosses_KEFD_Encalypta streptocarpa-2061474
Mosses_ZTHV_Atrichum angustatum-2048696
Mosses_HVBQ_Tetraphis pellucida-2131692
Mosses_ZQRI_Timmia austriaca-2067602
Mosses_YMXJ_Leucobryum albidum-2006570
Mosses_RDOO_Racomitrium varium-2003499
Mosses_WNGH_Aulacomnium heterostichum-2003799
Mosses_YWNF_Hedwigia ciliata-2005808
Mosses_BGXB_Plagiomnium insigne-2061681
Mosses_QKQD_Pseudotaxiphyllum elegans-2007533
Mosses_QKQD_Pseudotaxiphyllum elegans-2007534
Mosses_ZACW_Leucobrin brachypus-2048634
Mosses_JADL_Rhynchostegium serrulatum-2008912
Mosses_VBMM_Claopodium rostratum-2000940
Mosses_MRIS_Climacium dendroides-2088612
Mosses_WSPM_Loeskeobryum brevirostre-2005978
Mosses_AWOI_Diphyscium foliosum-2077066
Mosses_UHLI_Sphagnum recurvum-2094251
Mosses_ZTHV_Atrichum angustatum-2064674
Mosses_WOGB_Andreaea rupestris-2095021
Mosses_HVRG_Tetraphis pellucida-2008056
Mosses_HVBQ_Tetraphis pellucida-2095001
Mosses_SKQD_Takakia lepidozioides-2010746
Mosses_WOGB_Andreaea rupestris-2095603
Mosses_ZTHV_Atrichum angustatum-2084955
Mosses_GGWD_Sphagnum leucoti-2008657
Mosses_GGWD_Sphagnum leucoti-2008658
Mosses_HVBQ_Tetraphis pellucida-2019835
Mosses_AWOI_Diphyscium foliosum-2014805
Mosses_HRWG_Buxbaumia aphylla-2070345
Mosses_RGKI_Leucobryum glaucum-2005505
Mosses_GRKU_Syntrichia princeps-2017783
Mosses_ZQRI_Timmia austriaca-2004197
Mosses_BPSG_Scouleria aquatica-2021771
Mosses_JMXW_Bryum argenteum-2004957
Mosses_ORKS_Philonotis fontana-2002652
Mosses_CMEQ_Orthotrichum lyellii-2034910
Mosses_YWNF_Hedwigia ciliata-2009428
Mosses_WNGH_Aulacomnium heterostichum-2015534
Mosses_DHWX_Fontinalis antipyretica-2005899
Mosses_TNAJ_Neckera douglasii-2005689
Mosses_TNAU_Neckera douglasii-2005691
Mosses_WSPM_Loeskeobryum brevirostre-2008823
Mosses_QKQD_Pseudotaxiphyllum elegans-2050319
Mosses_JADL_Rhynchostegium serrulatum-2048101
Mosses_VBMM_Claopodium rostratum-2053406
Mosses_IGUH_Leucobryum julaceus-2020492
Mosses_ZACW_Leucobrin brachypus-2012335
Lc contig 6416
Liverworts_PIUF_Pellia sp. (cf epiphylla (L.) Corda)-2091366
Sm XP 002992796.1
Sm XP 002962749.1
Sm XP 002963396.1
Sm XP 002962783.1
Liverworts_FITN_Treubia lacunosa-2016439
Sm XP 002987792.1
Sm XP 002989916.1
Pt XP 006374329.1
OsPT11
Pt XP 006371312.1
Medtr5g080140.1
OsPT9
OsPT10
OsPT13
OsPT4
OsPT5
Hornworts_RXRQ_Phaeoceros carolinianus-2012579
OsPT8
OsPT12
OsPT6
OsPT7
OsPT3
OsPT1
OsPT2
Pt XP 006363466.1
Pt XP 002306623.2
Medtr1g043220.1
Medtr1g043290.1
Medtr1g043200.1
Medtr1g074080.1
Pt XP 002315705.1
Pt XP 006378341.1
Pt XP 006378342.1
Pt XP 002300153.2
Pt XP 006379240.1
Medtr1g074940.1
Pt XP 002306644.2
Pt XP 002306645.1
Pt XP 002302047.1
Medtr1g008035.1
Medtr1g069930.1
Medtr1g066870.1
Medtr1g068880.1
Liverworts_FITN_Treubia lacunosa-2091542
Hornworts_RXRQ_Phaeoceros carolinianus-2007404
Hornworts_WCZB_Phaeoceros carolinianus-2016787
Hornworts_FAJB_Paraphymatoceros hallii-2056323
Hornworts_DXOU_Anthoceros aenigmaticus-2036279
Hornworts_UCRN_Megaceros flagellaris-2053320
Hornworts_TCBC_Notothylas virgata-2009973
Hornworts_RXRQ_Phaeoceros carolinianus-2139629
Mosses_IGUH_Leucobryum julaceus-2016644
Mosses_ZACW_Leucobrin brachypus-2007766
Mosses_VBMM_Claopodium rostratum-2011454
Mosses_JADL_Rhynchostegium serrulatum-2000366
Mosses_WNGH_Aulacomnium heterostichum-2014762
Mosses_CMEQ_Orthotrichum lyellii-2012113
Mosses_JMXW_Bryum argenteum-2001201
Mosses_ORKS_Philonotis fontana-2011364
Mosses_YWNF_Hedwigia ciliata-2051323
Mosses_ABCD_Racomitrium elongatum-2011031
Mosses_RGKI_Leucobryum glaucum-2011012
Mosses_YMXJ_Leucobryum albidum-2004607
Mosses_KEFD_Encalypta streptocarpa-2061749
Mosses_BPSG_Scouleria aquatica-2021146
Mosses_ZQRI_Timmia austriaca-2016246
Mosses_YEPO_Physcomitrium sp.-2011487
Pty XP 001758324.1
Mosses_AWOI_Diphyscium foliosum-2072618
Mosses_HVBQ_Tetraphis pellucida-2022179
Mosses_RCBT_Sphagnum palustre-2031797
Mosses_HRWG_Buxbaumia aphylla-2010028
Pty XP 001781403.1
Mosses_DHWX_Fontinalis antipyretica-2074902
Pty XP 001784627.1
LpPT
Liverworts_TXYB_Lunularia cruciata-2074692
Liverworts_HERT_Sphaerocarpos texanus-2000301
Liverworts_IHWO_Marchantia paleacea-2006223
Liverworts_LFVP_Marchantia paleacea-2011355
Liverworts_WJLQ_Riccocarpos natans-2009119
Liverworts_HMHL_Marchantia paleacea-2010787
Liverworts_IHWO_Marchantia paleacea-2009687
Liverworts_HMHL_Marchantia paleacea-2011253
Liverworts_LFVP-Marchantia paleacea-2068236
Liverworts_IHWO_Marchantia paleacea-2067684
Liverworts_JPYU_Marchantia polymorpha-2005387
Lc 1311
Liverworts_ILBQ_Conocephalum conicum-2046421
Liverworts_WJLQ_Riccocarpos natans-2089893
Liverworts_JHFI_Pella neesiana-2019437
Liverworts_PIUF_Pellia sp. (cf epiphylla (L.) Corda)-2013761
Liverworts_YFGP_Pallavicinia lyellii-2108567
Liverworts_BNCU_Radula lindenbergiana-2018363
Liverworts_KRJQ_Porella navicularis-2013836
Liverworts_CrLU_Frullania spp.-2010168
Liverworts_TQKR_Frullania sp.-2014742
Liverworts_RTNU_Calypogeia fissa-2184038
Liverworts_LGOW_Schistochila sp.-2104644
Liverworts_HPXA_Plagiochila pulcherrima-2018453
Liverworts_NWQC_mixed species-2014567
Liverworts_RTNU_Calypogeia fissa-2017140
Liverworts_RTNU_Calypogeia fissa-2183460
Liverworts_WZYX_Barbilophozia hatcheri-2005270
Liverworts_YBQN_Odontoschisma prionitum-2129684
Green Algae_WOCW_Mesostigma viridicheinarium_proteins 9955
Green Algae_RPGL_Cylindrocystis brebissonii_proteins 10034
Green Algae_VAZE_Cylindrocystis sp._proteins 1762
Green Algae YLBK Cylindrocystis brebissonii-2 samples combined proteins 13749
Green Algae_YOIX_Cylindrocystis brebissonii_proteins 56002
Green Algae_VAZE_Cylindrocystis sp._proteins 1763
Green Algae YLBK Cylindrocystis brebissonii-2 samples combined proteins 43311
Green Algae_YOIX_Cylindrocystis brebissonii_proteins 8955
Green Algae_HKZW_Mesotaenium caldariorum_proteins 13878
Green Algae_MFZG_Zygnemopsis sp._proteins 28047
Green Algae_JOJQ_Cylindrocystis cushleckae_proteins 39066
Green Algae_HKZW_Mesotaenium caldariorum_proteins 803
Green Algae_HKZW_Mesotaenium caldariorum_proteins 804
Green Algae_JOJQ_Cylindrocystis cushleckae_proteins 4278
Green Algae_SNOX_Planctonium orbiani_proteins 3803
Green Algae_SNOX_Planctonium orbiani_proteins 3804
Green Algae_KMNX_Nucleotaenium eiffelense_proteins 37900
Green Algae_KMNX_Nucleotaenium eiffelense_proteins 38102
Green Algae_XRTZ_Roya obtusa_proteins 2577
Green Algae_KEYW_Gonatozygon kinahanii_proteins 1486
Green Algae_DRFX_Closterium lunula_proteins 1383
Green Algae_DRFX_Closterium lunula_proteins 1385
Green Algae_DRFX_Closterium lunula_proteins 1386
Closterium c14200 g1.i1
Green Algae_AEKF_Penium margaritaceum_proteins 12308
Green Algae_RPQV_Phymatodiscus nordstedtianus_proteins 36342
Green Algae_MNNM_Cosmarium granatum_proteins 3544
Green Algae_MNNM_Cosmarium granatum_proteins 3545
Green Algae_ISKC_Staurastrum setiaki_proteins 9772
Green Algae_RPRU_Staurodesmus omearii_proteins 42822
Green Algae_GYSP_Euastrum affine_proteins 205545
Green Algae_WCGU_Staurodesmus convergens_proteins 9412
Green Algae_BHBK_Cosmarium tinctum_proteins 50530
Green Algae_RQFE_Cosmocladium cf. constrictum_proteins 37606
Green Algae_MCHJ_Micrasterias fimbriata_proteins 8722
Green Algae_WGGV_Cosmarium subtumidum_proteins 55958
Green Algae_MOYY_Pleurotaenium trabecula_proteins 10767
0.1

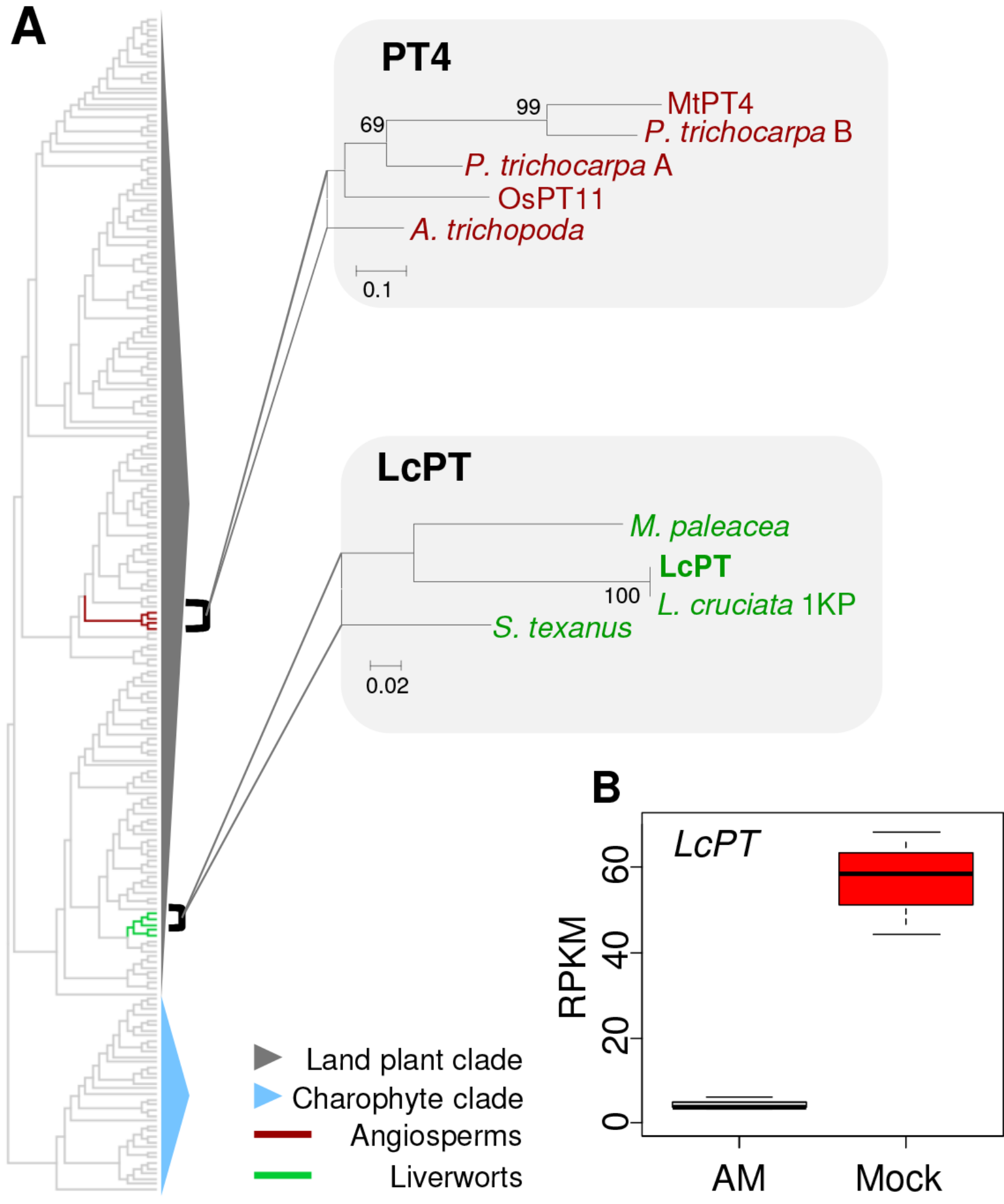
A
PT4
99
69
MtPT4
P. trichocarpa B
P. trichocarpa A
OsPT11
A. trichopoda
0.1
LcPT
M. paleacea
LcPT
100
L. cruciata 1KP
S. texanus
0.02
B
LcPT
RPKM
0
20
40
60
AM
Mock
Land plant clade
Charophyte clade
Angiosperms
Liverworts

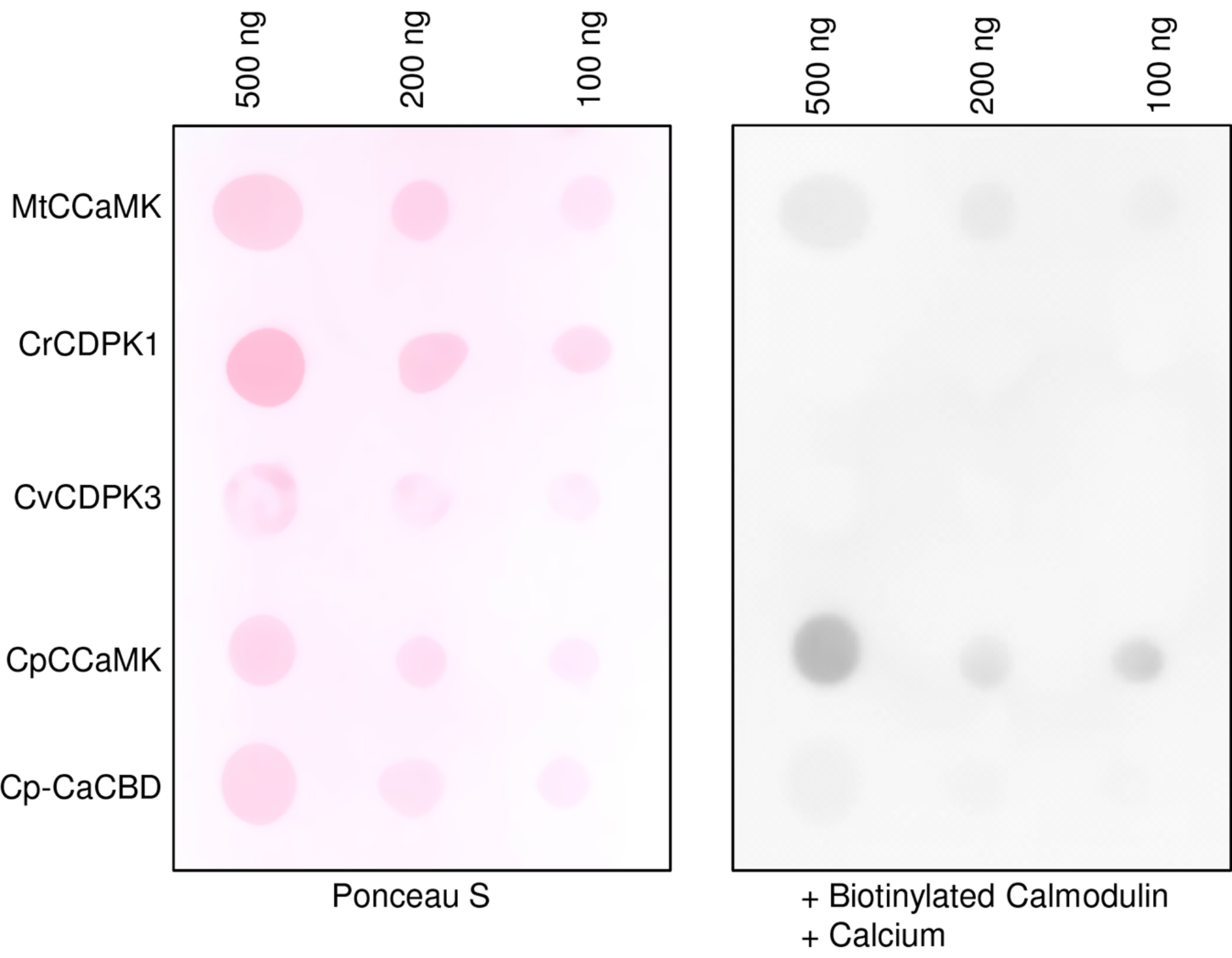
500 ng
200 ng
100 ng
500 ng
200 ng
100 ng
MtCCaMK
CrCDPK1
CvCDPK3
CpCCaMK
Cp-CaCBD
Ponceau S
+ Biotinylated Calmodulin
+ Calcium

A

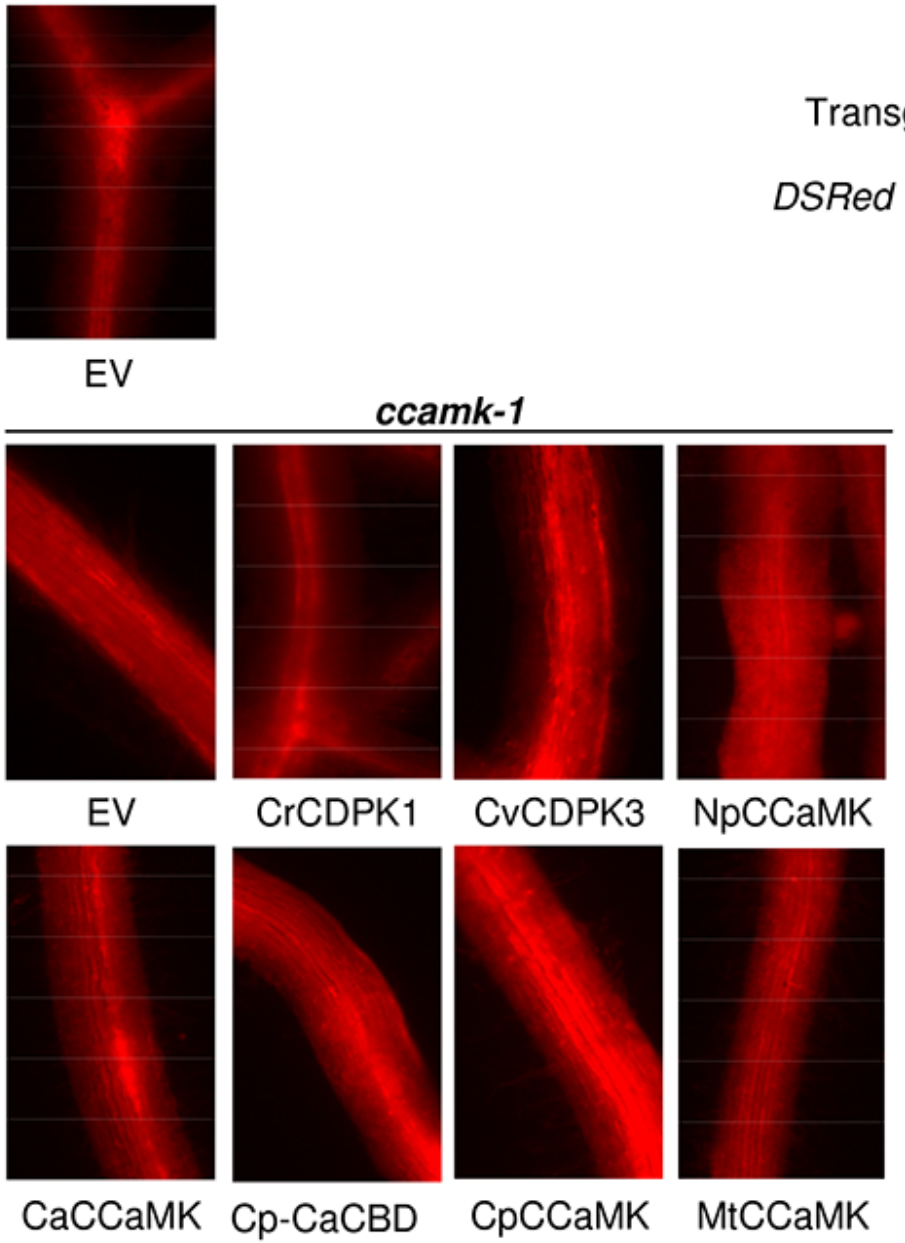

B

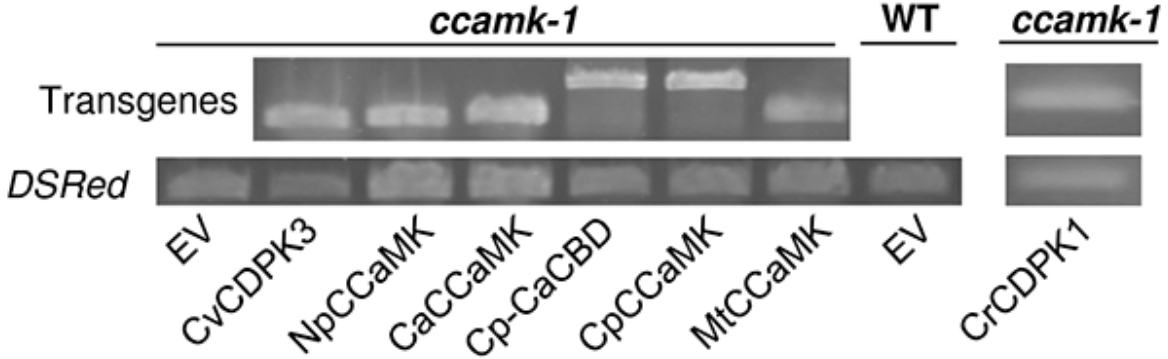

C

CrCDPK1-F	5'- AGGACAAGAGCGGCTTCATA
CrCDPK1-R	5'- ACGACCACCTTGGTCTTGAG
CvaCDPK3-F	5'- CAGAGTATGAGCGGGACACA
CvaCDPK3-R	5'- TTCGGGCTTGAGATCTCTGT
CpCCaMK-F	5'- ATGGGCGACGTGGAGGAG
CpCCaMK-R	5'- CACCTCAGGCTCCATCG
CaCCaKM-K-F	5'- AACCTCATCCGTCTGCTCAA
CaCCaKM-K-R	5'- CAACGAGCCAAACAGACCAA
NpCCaMK-F	5'- ATGTCGCGCTCATCAGAAAC
NpCCaMK-R	5'- CGGGGTTTCAAACAGCATGT
MtDMI3-F	5'- GACTGAAGCTGCAACTGTGG
MtDMI3-R	5'- TTTGGGCAATGAAAGGTGGA
DSRed-F	5'- ACGAAGGCCACAATACCGTA
DSRed-R	5'- CCACCGTCTTTCAGCTTCAG